



Universidade Federal
do Rio de Janeiro

Escola Politécnica

Effects of Process Parameters Joining the dissimilar materials AA6082-T6 and AISI 316Ti by Friction Stir Welding

Victor Mello Callil

Projeto de Graduação apresentado ao Curso de Engenharia Naval e Oceânica da Escola Politécnica, Universidade Federal do Rio de Janeiro, como parte dos requisitos necessários à obtenção de título de Engenheiro

Orientador(es): Jean David Job E.M.Caprace
Luciano Andrei Bergmann
Marcelo Igor L. de Souza

Rio de Janeiro
Janeiro de 2020

FSWed DISSIMILAR ALUMINIUM/STEEL MATERIALS 6 mm
THICK IN BUTT JOINT CONFIGURATION

Victor Mello Callil

PROJETO DE GRADUAÇÃO SUBMETIDO AO CORPO DOCENTE DO CURSO DE ENGENHARIA NAVAL E OCEÂNICA DA ESCOLA POLITÉCNICA DA UNIVERSIDADE FEDERAL DO RIO DE JANEIRO COMO PARTE DOS REQUISITOS NECESSÁRIOS PARA A OBTENÇÃO DE GRAU DE ENGENHEIRO NAVAL.

Examinado por:

Prof. Jean David Job E.M.Caprace

Prof. Marcelo Igor L. de Souza

Prof. Murilo A. Vaz

Prof. Julio Cesar R. Cyrino

RIO DE JANEIRO, RJ – BRASIL
JANEIRO DE 2020

Callil, Victor Mello

FSWed dissimilar aluminium/steel materials 6 mm thick in butt joint configuration / Victor Mello Callil – Rio de Janeiro: UFRJ/Escola Politécnica, 2018.

Xii, 44 p.: il; 29,7 cm.

Orientador(es): Jean-David J. E. M. Caprace

Luciano Andrei Bergmann

Marcelo Igor L. de Souza

Projeto de Graduação – UFRJ / Escola Politécnica / Curso de Engenharia Naval e Oceânica, 2018.

Referências Bibliográficas: p 58-61.

1. FSW 2. Dissimilar Joints 3. Butt joint configuration
4. Experimental Tests 5. AISI 316 Ti / AA 6082 – T6

I. Caprace, Jean David *et al.* II. Universidade Federal do Rio de Janeiro, Escola Politécnica, Curso de Engenharia Naval e Oceânica III. FSWed dissimilar aluminium/steel materials 6 mm thick in butt joint configuration

AGRADECIMENTOS

Gostaria de agradecer e dedicar esta dissertação às seguintes pessoas:

Minha Família, minha mãe Denise, meu pai Mauro, minha irmã Thais e minhas avós Maria e Lourdesy, pelo suporte único a que me foi proporcionado durante todo o período de universidade.

Meus orientadores Luciano Bergmann, Jean-David Caprace e Marcelo Igor de Souza, pela expertise habitual e contribuição valorosa para este trabalho.

Minha namorada Juliana e sua família, por todo o carinho demonstrado durante toda a jornada.

Meus amigos da universidade Ryan Coutinho, Felipe Pereira, Rafaela Valença, Danielle Carneiro, Caio Bertolo, Leonardo Silva, Nicholas Dutra, George Honorato, Vitor Carone e tantos outros que, de alguma forma, contribuíram para que este trabalho fosse executado.

Meus amigos do HZG Stefano, Natan, Renan, Milli, Joana, Bruno, Rasmus, Fábio, Jonas, William e todo o departamento do WMP, por todo o suporte e amizade durante o ano de 2017.

Enfim, agradeço a todas as pessoas que fizeram parte dessa etapa decisiva em minha vida.

ESTÁGIO

Assim como para a grande maioria dos estudantes universitários, o intercâmbio acadêmico sempre foi um de meus objetivos desde minha entrada na universidade. Ainda mais em um mundo globalizado e competitivo, uma experiência fora do país sempre aparece como uma ferramenta de especialização e oportunidades únicas de conhecimento. Porém, esse objetivo ficou mais distante a partir do corte de bolsas do programa “Ciência sem fronteiras”. Mesmo assim, através da persistência e busca incessante por uma oportunidade, o objetivo fora alcançado e consegui o estágio na Alemanha, em Fevereiro de 2017, onde permaneci até o fim do mesmo ano.

A parte técnica do assunto ainda era desconhecido: Solda por Fricção de chapas dissimilares. Através de revisões de literatura e ajuda dos colegas de departamento, fui me interessando pelo assunto e percebi o grande potencial da soldagem em estado sólido para o ambiente naval: a junção mecânica de chapas de aço e alumínio de casco e convés, respectivamente.

Além da parte técnica envolvida, o ambiente (completamente distinto do Brasil) contribuiu para meu crescimento pessoal e profissional. As idas e vindas de bicicleta e os passeios aos fins de semana aumentaram meu rendimento e concentração nos dias de semana, e percebi uma melhora significativa de como utilizar melhor meu tempo. Os desenvolvimentos das línguas inglesa (principalmente) e alemã serão de grande valia para meu futuro profissional. As amizades e a ética profissional levarei sempre comigo, assim como o aprendizado fantástico ao longo desses 10 meses, nos âmbitos profissional e pessoal

Resumo do projeto de Graduação apresentado à Escola Politécnica / UFRJ como parte integrante dos requisitos necessários para a obtenção de grau de Engenheiro Naval

FSWed dissimilar Aluminium/Steel materials 6 mm thick in butt joint configuration

Victor Mello Callil

Janeiro/ 2020

Orientador(es): Jean-David J. E. M. Caprace

Luciano Bergmann

Marcelo Igor L. de Souza

Curso: Engenharia Naval e Oceânica

Estaleiros construtores de Navios Cruzeiro e Roll-On Roll-Off vêm adotando, em todo o mundo, juntas de aço/alumínio fabricados pelo método de explosão como solução à soldagem de chapas de aço e alumínio de casco e convés, respectivamente. Embora utilizado na indústria naval, tal método apresenta baixas propriedades mecânicas, alta emissão de CO₂, alto custo de produção e segurança de construção questionável.

A função do presente trabalho consiste em apresentar o método de Friction Stir Welding (FSW) como alternativa de soldagem de junta aço / alumínio, deixando claro os resultados obtidos e comparando-os com as propriedades mecânicas da solda por explosão. As chapas de aço e alumínio foram dimensionadas com 300 mm de comprimento, 150 mm de largura e 6 mm de espessura (300 x 150 x 6 mm) foram posicionados em configuração de solda de topo com a ferramenta deslocada para o lado do alumínio de modo a evitar o desgaste do pino (*probe*) da ferramenta. Os melhores resultados foram obtidos para um offset de 0,1 mm, com velocidade rotacional de 300 RPM, 2,0 mm/s de velocidade de translação, 12,5 KN de força axial e 1° de ângulo de inclinação, onde tensão máxima admissível (UTS) atingiu 62,73% da tensão máxima do alumínio, enquanto a tensão máxima atingida para solda por explosão chega a cerca de 24,19% do tensão máxima do alumínio. Tal expertise atuando como um todo na indústria naval pode mudar os rumores e metodologia de construções navais com a implementação do método FSW para juntas dissimilares aço/alumínio, devido às altas propriedades mecânicas atingidas, acurácia de fabricação e menor custo.

Abstract of Undergraduate Project presented to DEMM / POLI / UFRJ as a partial fulfillment of the requirements for the degree of Naval Engineer.

FSWed dissimilar Aluminium/Steel materials 6 mm thick in butt joint configuration

Victor Mello Callil

January/ 2020

Advisor(s): Jean-David J. E. M. Caprace

Luciano Bergmann

Marcelo Igor L. de Souza

Course: Naval and Ocean Engineering

Worldwide, shipyards manufacturers of cruise and roll-on/roll-off vessels worldwide have adopted steel-aluminium joints made by the explosion method to fasten steel plate of the hull to the aluminium plates of the decks. Although this methodology is used in naval field, it presents weak mechanical properties, CO₂ emission, high cost production and low manufacturing safety. The purpose of this work is to analyse the effects of process parameters joining the dissimilar materials AA6082 and AISI316 by Friction Stir Welding (FSW) and to compare them to the mechanical properties obtained by the explosion bonding technique. Both the aluminium and steel plates were 300 x 150 x 6 mm, laid out in butt-joint configuration with tool displaced towards the aluminium sheet in order to prevent wear of the probe. The best results were obtained for an offset of 0.1 mm with a 300 RPM rotation speed, 2.0 mm/s translation speed, 12.5 KN axial force and 1° tilt angle. The ultimate tensile strength achieved 62.73% of the aluminium base material, while the maximum tensile strength of explosion welding corresponds to 24.19% of the aluminium plate. These results may help improve the manufacturing techniques of marine structures, with FSW as one of the possible future joining techniques of dissimilar materials

ÍNDICE DE FIGURAS

Figure 1: 4-step procedure of FSW	3
Figure 2: FSW sketch displaying the-parameters involved: rotation speed, translation speed and axial force	4
Figure 3: Sketch of FSW parameters including rotation speed, translation speed, offset, axial force and tilt angle	6
Figure 4: Most used tool parts: Scrolled Shoulder and Threaded Probe	7
Figure 5: FSW top view - Onion Ring Formation	8
Figure 6: Weld Zones. The legend includes the SZ, TMAZ, HAZ and BM	9
Figure 7: Chart flow displaying the procedure adopted	18
Figure 8: Probe, shoulder and assembly	19
Figure 9: Main dimensions of steel and aluminium sheets.....	20
Figure 10: Joint configuration with 12° angle of the probe edge	20
Figure 11: Clamping system	22
Figure 12: Gantry system for FSW	22
Figure 13: Thermocouples arrangement in transversal and longitudinal views, respectively	23
Figure 14: Cut-off machine	24
Figure 15: Leica optical microscope.....	25
Figure 16: Grinding and polishing machine	25
Figure 17: Microhardness machine	26
Figure 18: Draft of Bending test including specimen, plunger on the top and dies on the bottom (support of the specimens)	27
Figure 19: Draft of TT specimen	27
Figure 20: Example of TT showing the specimen clamped on the grips and the extensometer located on the front surface of the FSW sample	28
Figure 21: SEM machine	29

Figure 22: Top view of the weld seam for all experiments	31
Figure 23: Temperature variation along time for thermocouples T2 up to T11 with temperature in Celsius and time in seconds	32
Figure 24: Aluminium and steel microstructure of welded joint in experiment E6	34
Figure 25: SEM pictures at the upper part of the joint corresponding to experiments E6, E7, E8 and E9	36
Figure 26: SEM pictures of the middle part of the joint corresponding to experiments E6, E7, E8 and E9	37
Figure 27: Steel inserts and precipitates within AA 6082-T6	37
Figure 28: Microhardness Vickers across the welded joint interface where left side is Aluminium and right-side Steel – (a) E6 to E9 and (b) E4 and E5	39
Figure 29: Tensile tests chart for experiments E4, E5, E6, E7, E8 and E9	41
Figure 30: Fracture position of Tensile test: Al side for E6 and E7 and joint line for E8 and E9	44

ÍNDICE DE TABELAS

Table 1: Wrought aluminium alloys designation system	11
Table 2: Temper designations.....	12
Table 3: Chemical composition AA 6082 - T6	13
Table 4: Mechanical properties AA6082 - T6.....	13
Table 5: Chemical composition AISI 316Ti.....	15
Table 6: Mechanical properties AISI 316Ti	16
Table 7: Diffusion elements.....	17
Table 8: Parameters applied in FSW samples	21
Table 9: Grinding and polishing clothes used in FSW samples	24
Table 10: Peak temperatures for thermocouples related to experiment E7	33
Table 11: EDS analysis for spots 1 and 7	38
Table 12: Tensile test results with Toughness and UTS.....	42
Table 13: Comparison between best FSW parameters and Triplate [®] Shockwave Metalworking Technologies BV	43
Table 14: Bending test results.....	43

Table of Contents

1	Introduction	1
2	Literature Review	3
2.1	FSW parameters.....	4
2.1.1	Rotation and translation speed	5
2.1.2	Axial Force and Plunge Depth	5
2.1.3	Tilt Angle	5
2.1.4	Offset.....	6
2.1.5	FSW Tool.....	6
2.2	Material Flow and Onion Ring Formation	7
2.3	Welding Zones	8
2.3.1	Stir Zone.....	9
2.3.2	Thermo-mechanical affected zone	9
2.3.3	Heat affected zone.....	9
2.4	Aluminium and Aluminium Alloys	10
2.4.1	General features	10
2.4.2	Alloy Designations.....	10
2.4.3	Wrought Alloys Designation System.....	11
2.4.4	Aluminium Temper Designations System	11
2.4.5	AA6082 – T6	13
2.5	Steel and Stainless steel	14
2.5.1	General Features	14
2.5.2	Steel Designations.....	14
2.5.3	AISI 316Ti	15
2.6	Aluminium/Steel and diffusion bonding.....	16
3	Experimental Approach.....	18

4	Materials and Methods	19
4.1	Materials	19
4.2	Methodology	20
4.2.1	Tool Configuration.....	20
4.2.2	Parameters study	21
4.2.3	FSW Machinery	22
4.2.4	Microstructure characterization	23
4.2.5	Microhardness characterization	25
4.2.6	Bending and tensile tests.....	26
4.2.7	Scanning Electron Microscope (SEM)	29
5	Results and discussions	30
5.1	Weld surface	30
5.2	Temperature distribution.....	32
5.3	Microstrucuture.....	33
5.4	Interface	34
5.5	Composition of the stir zone.....	37
5.6	Microhardness profile across the interface	38
5.7	tensile test and toughness.....	40
5.8	Bending test	41
5.9	Comparison with Triplate®	42
6	Conclusion.....	45
7	References	46

GLOSSARY

AS	advancing side
BM	base material
BT	bending test
EDS	energy dispersive X-ray spectrometry
FESEM	field emission scanning electron microscope
FSSW	friction stir spot welding
FSW	friction stir welding
HAZ	heat affected zone
IMC	intermetallic compound
NS	not specified
RFSSW	refill friction stir spot welding
RS	retreating side
SEM	scanning electron microscope
SZ	stir zone
TMAZ	thermomechanical affected zone
UTS	ultimate tensile strength

1 INTRODUCTION

Recently, there have been significant advances in shipbuilding construction. The growth in the demand of Cruise ships over the past decades required skilled labour to produce such ships in large scale. Inherent to these ships, stability and weight reductions have become major concerns among engineers due to significant amount of decks above the hull, e.g. the Symphony of the seas, currently the largest cruise ship of the world presents an air draught of 70 m. Embedding aluminium in the decks and steel in the hull maintains a good structural behavior in the bottom and lowers the center of gravity of the ship, reducing the stability issues.

In shipbuilding, aluminium-steel joining is generally performed by explosion method patented by Triplate® Shockwave Metalworking Technologies BV. The material consists in three layers of St 52-3N, aluminium-Mg4.5Mn and AA-1050A, used as intermediate layer to facilitate bonding between steel and aluminium alloy.

Although widely applied in industry, explosion techniques require high preparation time, special in-house conditions and specific outfit to carry out the explosion. Besides, ordinary drawbacks are produced including emission of CO₂ to the atmosphere and low mechanical properties of the joint. Nevertheless, key challenges must be addressed in order to find new ways of steel-aluminium joining for cost reduction and improvement of the mechanical properties. Advances in joining dissimilar materials have been taking place since last decade. Solid-state joining processes like FSW, FSSW and RFSSW have become scopes of academic research. Among them, FSW has been recently applied in industry, (Wang, Zhao, & Hao, 2018) and (Haghshenas & Gerlich, 2018), and it is known for its capacity of welding dissimilar materials producing high quality joints with good mechanical properties, (Y. Helal, 2019) and (Y. Huang, 2019).

In terms of shipbuilding, aluminium stiffened panels have been using FSW to join the stiffeners to the panel. But for dissimilar materials like steel-aluminium joint, FSW is still a gap to be deeply studied.

In accordance with the above information, this work aims to evaluate FSW dissimilar alloys regarding its mechanical properties and compare the obtained results with the results of Triplate® explosion welding. The implementation of FSW is directly

related to the market trend, where quality and effectiveness have been increasing the need of skillful labour and time saving in ship manufacturing.

2 LITERATURE REVIEW

Friction Stir Welding (FSW) is a solid-state joining process established by Wayne Thomas in 1991, in United Kingdom. FSW brings on high quality welds and high strength joints with low distortions. Such process is able to weld-plates in butt or overlapping configurations in a wide range of materials thicknesses using non-consumable tools.

The process is divided in four steps: **step 1**, the tool is placed above the plates where rotation speed and axial force are applied in order to plasticize the material and penetrate into the workpieces (**step 2**). After penetration, tool is able to move forward and produce the weld seam via heat generation and plastic deformation (**step 3**). When tool achieves the end, it moves out of the workpiece by an upward movement (**step 4**). The 4-step procedure is shown in Figure 1.

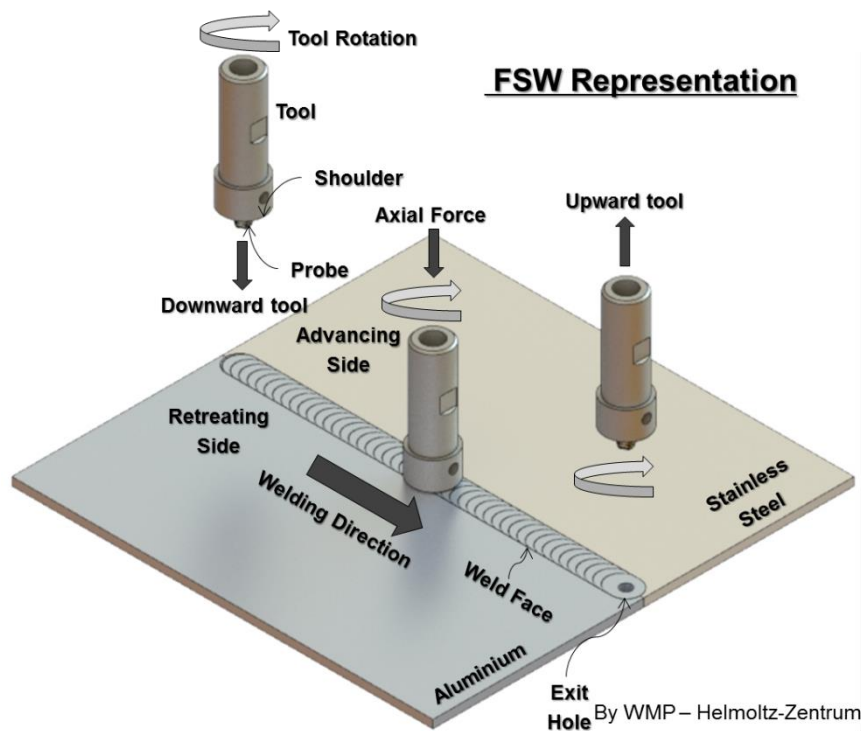


Figure 1: 4-step procedure of FSW

Special attention should be drawn in the distance between the probe and the backing bar. If the distance is too small, the probe can get in contact with the backing bar, leading waste of energy, wear of the probe and jam of the probe into the backing bar. If the distance is too big, heat generation will not be enough to lead heat generation in the bottom.

Besides, (Scupin, 2015) points out that the plunge depth of the probe is led by the combination between the axial force, rotation speed and translation speed. Thereby, the choice of welding parameters must be done carefully and based on previous experiences. It is important to emphasize that in FSW, the axial force varies along time leading variation of the plunge depth. Such oscillating force may cause non-uniform distribution of the heat and defects along weld line. Besides, excessive force pushes plasticized material out of the weld seam which is distributed along the borders of the weld seam. Such effect is known as *flash generation* in FSW theory. In Figure 2 is shown a draft of a FSW tool applied to aluminium/steel joint.

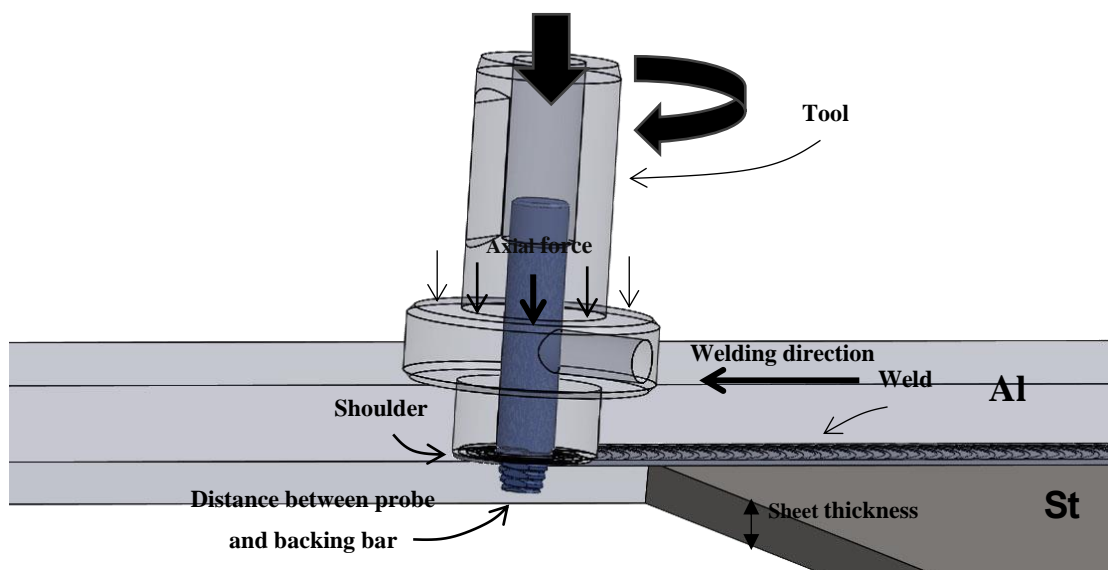


Figure 2: FSW sketch displaying the-parameters involved: rotation speed, translation speed and axial force

(R.S.Mishra, 2005) points out there are six major parameters that lead the quality of FSW. They are rotation speed, translation speed, axial force & plunge depth, tilt angle, offset distance and tool geometry. Each of them and their influence in the weld performance are explained in the Section 2.1.

2.1 FSW PARAMETERS

FSW involves complex material flow and weld formation. Welding parameters and tool geometry have crucial role on heat generation, material flow, plunge depth and temperature distribution along the weld seam.

2.1.1 ROTATION AND TRANSLATION SPEED

Rotation and translation speed are parameters that must be considered during FSW. The choice of these parameters must be done prior to weld because both parameters influence the weld properties. If rotation speed is too high, heat generation will increase. If rotation speed is low, heat generation will decrease. The other way around works for translation speed. If speed is too high, less heat will be led. If speed is too low, more heat will be generated.

The material surrounding the tool should be hot enough to enable plastic flow required by FSW, which depends basically on the material and rotation / translation speed. If the material is too cold (low rotation speed / high translation speed), voids and flaws may show up in the SZ, which leads significant brittleness within it. In the other hand, excessive heat (high rotation speed / low translation speed) input may either dissolve aluminium precipitates or even melt it depending on temperature occurred.

2.1.2 AXIAL FORCE AND PLUNGE DEPTH

Axial force is the parameters responsible for controlling the plunge depth. The higher force applied, the higher plunge depth and heat generation will be. The choice of axial force is an important task in order to ensure the quality of the weld and safety of the equipment involved in FSW. If the force is too high, heat input may increase and lead flash generation, as well as reducing SZ area. As mentioned in Section 2, axial force must be set constant during FSW to keep same distance between bottom of the probe and the backing bar. Some FSW machines are operated under load control, which is the case of this work.

In order to prevent tool wear and tear, the probe was checked after welding to make sure that the it has not been worn out during the process.

2.1.3 TILT ANGLE

Another important process parameter is the tilt angle or angle of spindle with respect to the workpiece surface. The tilt angle is measured with regard to the tool centerline. According to (R.S.Mishra, 2005), a suitable tilt angle towards trailing edge ensures that the shoulder holds the stirred material underneath it and concentrates the heat locally.

2.1.4 OFFSET

The probe is a steel manufactured pin of the tool subjected to rotation and translation speed. If probe penetrates or even rubs steel sheet during FSW, it can get worn out leading to waste of material and low weld quality. Thereby, the probe must keep a constant distance from the steel plate. In literature, this distance is called offset. The higher the offset, the lower the wear of the probe. If offset is low, probe wear is higher. In Figure 3, the offset is illustrated in details.

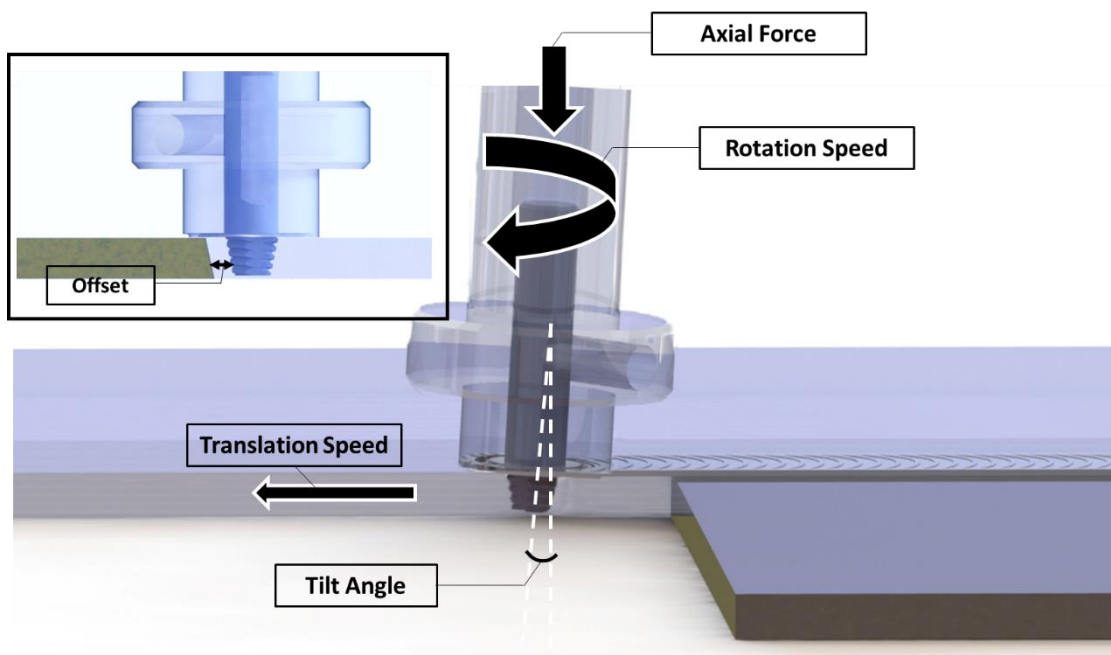


Figure 3: Sketch of FSW parameters including rotation speed, translation speed, offset, axial force and tilt angle

2.1.5 FSW TOOL

Tool geometry is one of the most important aspects of FSW performance. FSW tool consists of a probe and shoulder attached together. The sketch is shown in Fig. Figure 4. According to (R.S.Mishra, 2005), the tool has two major roles: (a) localize the heat, which most part of it is governed by the shoulder and (b) material flow.

In FSW, it is usual to use scrolled shoulder attached to threaded probe. (W.M, E.D.Nicholas, & S.D.Smith, 2001) points out threaded pins are shaped to displace less material than a cylindrical probe. Such tool design is believed to (a) reduce welding forces, (b) enable easier flow of plasticized material, (c) increase interface between plasticized material which increases heat generation and (d) decrease the displaced

volume of material from the AS to the RS. In the upper part of the plate, heat generation is even higher, since shoulder stirs the upper region of the welded plates.

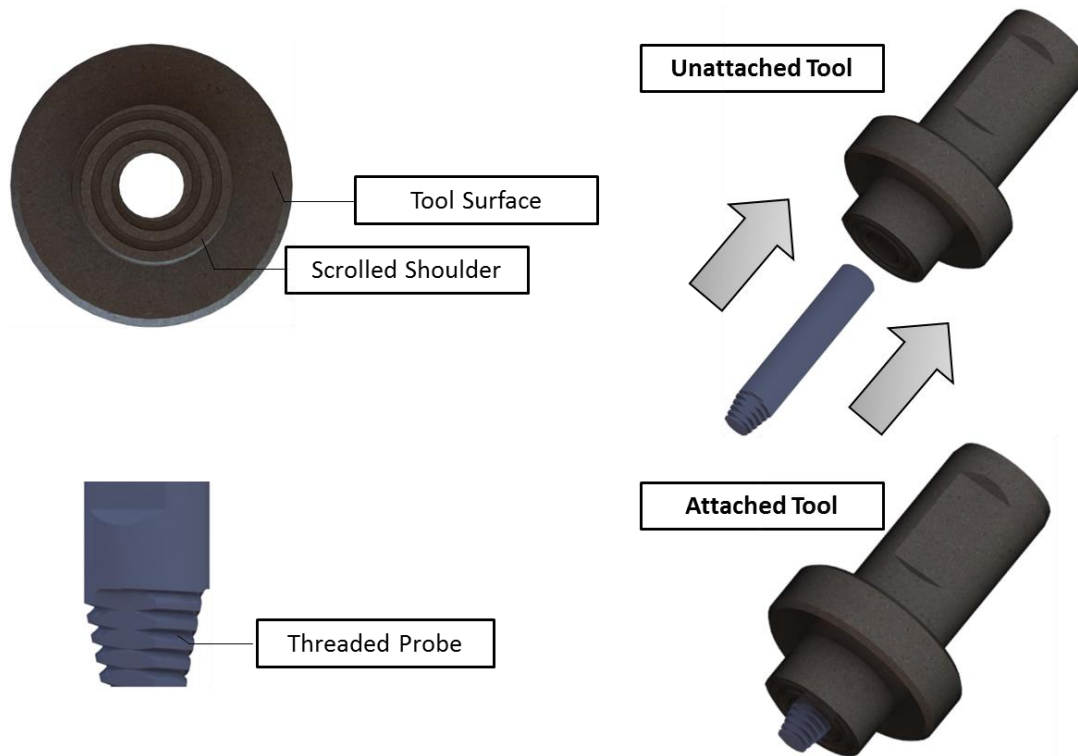


Figure 4: Most used tool parts: Scrolled Shoulder and Threaded Probe

2.2 MATERIAL FLOW AND ONION RING FORMATION

In a butt joint configuration, the sheets are placed side-by-side and rotation direction and rotation movement determinates AS and RS. The determination of AS and RS are significant in FSW because they influence on onion ring formation, material flow and temperature distribution.

The onion ring formation is a multi-layered deposition of metal. (S.Muthukumaran & Mukherjee, 2007) points out that “onion” movement takes place from the AS to the RS. When tool is rubbing AS, the contact pressure is high. As long as tool moves towards RS, such pressure drops down below a critical value. By the time material reaches the rear side, it is deposited at RS. However, as far as tool moves towards AS the contact pressure increases again. Such phenomena take place over and over until

FSW is finished. The deposition of different layers characterizes FSW as a multi-layered deposition process that is repeated as long as the tool moves to the end.

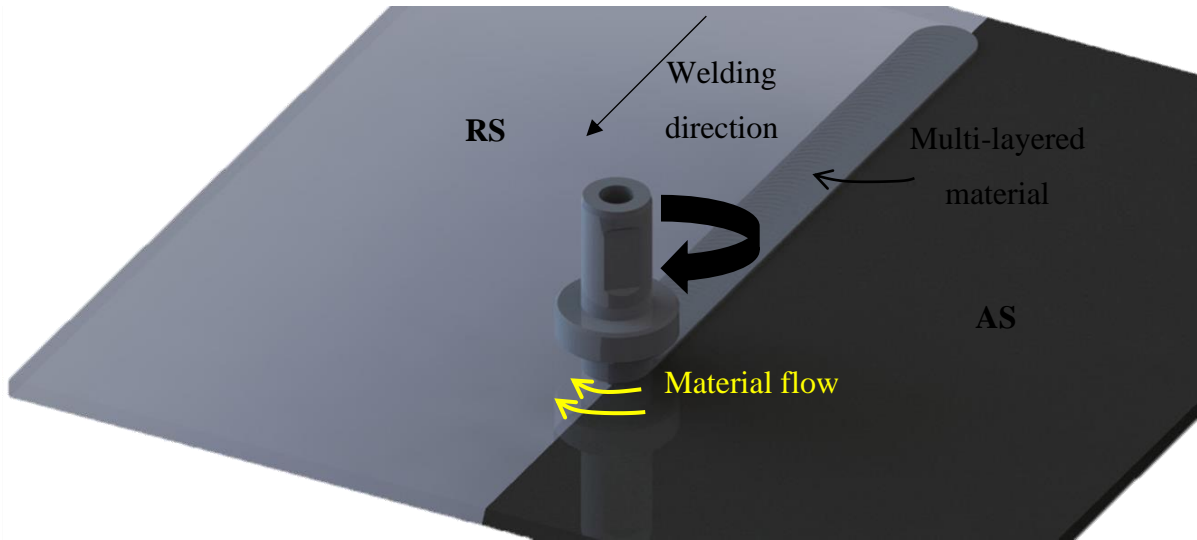


Figure 5: FSW top view - Onion Ring Formation

The rotational speed starts when tool is settled on the AS, where material is non-deformed. As mentioned by (S.Muthukumaran & Mukherjee, 2007), the contact pressure is greater when the tool is in the AS. As far as the tool approaches the RS, the material is deposited there. The non-deformed material in AS may undergo high energy and contact pressure. Meanwhile, the already deformed material will undergo lower energy and contact pressure when achieving RS. Such energy difference between AS and RS makes the temperature in AS higher than in RS. Thereby, it is reasonable to affirm that temperature in AS is slightly higher than in RS considering two fully identical plates.

2.3 WELDING ZONES

In Section 2.2, we pointed out that temperature in the AS is slightly higher than in RS, supposing same material for both sheets. In FSW, it is really common and widely approached the concept of welding zones. They are known as stir zone (SZ), thermo-mechanical affected zone (TMAZ) and heat affected zone (HAZ). The arrangement of the weld zones is described in the next topics and shown in Figure 6.

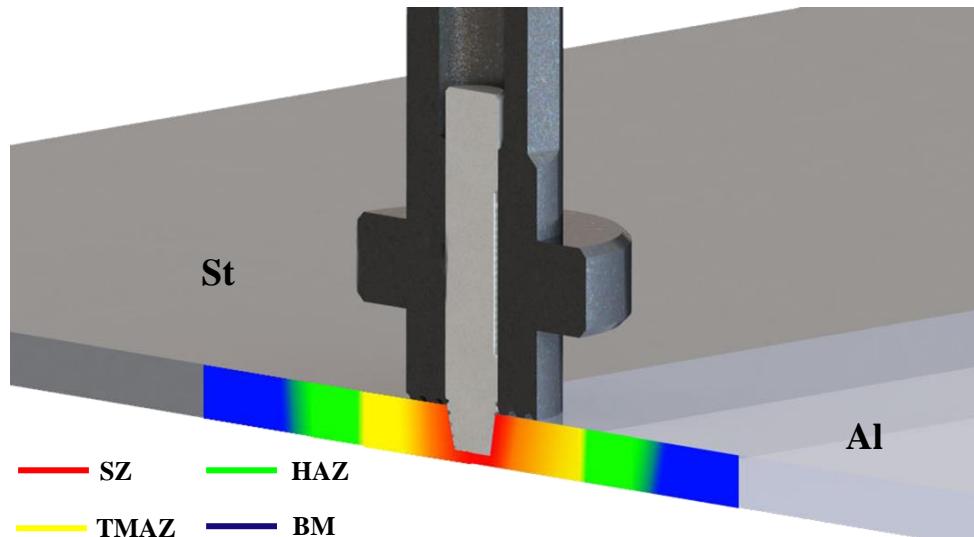


Figure 6: Weld Zones. The legend includes the SZ, TMAZ, HAZ and BM

2.3.1 STIR ZONE

Intense plastic deformation and friction leads to dynamic recrystallization of fine grains within SZ microstructure. In dynamic recrystallization, as opposite of static recrystallization, nucleation and growth of new grains occurs during deformation rather than afterwards as part of a separate heat treatment. FSW parameters (described in Section 2.1), material composition and temperature have great influence on grain size after recrystallization. The region can be referred either as stir zone (SZ) or dynamic recrystallization zone (DRZ).

2.3.2 THERMO-MECHANICAL AFFECTED ZONE

TMAZ is located between SZ and HAZ. TMAZ undergoes high temperature and plastic deformation-and can be easily identified because its grains are generally deformed in the same direction, i.e. there is pattern deformation of the grains. Although TMAZ undergoes plastic deformation, dynamic recrystallization does not take place due to low deformation strain; the opposite situation occurs in SZ. However, since TMAZ undergoes high temperature, precipitates can be dissolute depending on the degree of temperature and deformation.

2.3.3 HEAT AFFECTED ZONE

HAZ is located right after TMAZ. Such region undergoes thermocycles along FSW however with no plastic deformation taking place. Thereby, neither dynamic recrystallization nor plastic deformation takes place in HAZ. The high temperature

undergone by HAZ leads overgrowth of the grains. These big grains may generate dislocations in different spots of HAZ. If the number of dislocations is meaningful, HAZ may be considered a fragile zone, where fractures and cracks can be increased by an initial deformation in mechanical experiments.

2.4 ALUMINIUM AND ALUMINIUM ALLOYS

2.4.1 GENERAL FEATURES

This raw material can be obtained from bauxite, an ore that can be found in three major climatic groups: Mediterranean, tropical and subtropical. Bauxite should be containing at least 30% of aluminium oxide (Al_2O_3) in order to become the production economically feasible.

Aluminium is a soft, durable, lightweight and ductile metal with appearance that ranges from silvery until dull gray, depending on the surface roughness. It is non-magnetic and does not ignite too easily. The yield strength of pure aluminium ranges from 7 up to 11 MPa as long as aluminium alloys have yield strengths varying from 200 MPa up to 600 MPa. Aluminium has about one third the density and stiffness of steel. Besides, it can be easily machined, cast or extruded.

Besides, aluminium is a good thermal and electrical conductor, over 1062% of steel conduction value. Aluminium is capable of superconductivity, with a superconducting critical temperature of 1.2 K and a critical magnet field of about 100 Gauss.

Back in the forty's (1940's), application of aluminium in constructions and architecture was not quite plentiful. The metal was mainly used to produce airplanes. However, in the middle of twentieth century, aluminium has become more popular in construction of skyscrapers and bridges. Window frames, ships, boats, panels, domed roof and wide-span constructions have been increasingly aluminium manufactured.

2.4.2 ALLOY DESIGNATIONS

The alloy designations are set according to (Association, 2015) responsible for the allocation and registration of aluminium alloys. Currently, there are over 400 wrought alloys and wrought aluminium alloys and over 200 aluminium alloys on form of casting. Aluminium alloys can be listed into a number of groups based on a particular material's features such as its ability to respond to thermal and mechanical treatment.

2.4.3 WROUGHT ALLOYS DESIGNATION SYSTEM

We shall consider the first 4-digit wrought aluminium alloy identification system. The first digit (Xxxx) indicates the main alloying element, which has been added to the aluminium alloy and is often used to describe the aluminium series, i.e., 1000 series, 2000 series, 3000 series up to 8000 series. The second digit, if different from 0, indicates a modification on a specific alloy. The third and fourth digits are arbitrary numbers provided to identify a specific alloy of the series. An example is AA 6082, where 6 indicates content of magnesium and silicon, 0 non-modified alloy and 82 is the ID number. Table 1 the respective designations of each alloy according to (Association, 2015).

Table 1: Wrought aluminium alloys designation system

<i>ALLOY SERIES</i>	<i>MAJOR ALLOYING ELEMENTS</i>
1xxx	99.000% Minimum Aluminium
2xxx	Copper
3xxx	Manganese
4xxx	Silicon
5xxx	Magnesium
6xxx	Magnesium and Silicon
7xxx	Zinc
8xxx	Other alloying elements

Source: (AlcoTec, 2015)

2.4.4 ALUMINIUM TEMPER DESIGNATIONS SYSTEM

Basing the knowledge on aluminium designations and their meanings, it is noticeable the difference of their characteristics and consequent applications. After understanding alloying nomenclature, we should identify whether alloy is heat treatable or not. 1xxx, 3xxx and 5xxx wrought aluminium alloys are considered non-heat treatable alloys. 2xxx, 6xxx, 7xxx wrought aluminium series are considered wrought heat treatable alloys.

Heat treatment aims at improving mechanical properties through a process of thermal treatment. The most usual is solution heat treated and artificially aged afterwards. Solution heat treatment is the process where the alloys is heat up to a temperature close

to fusion temperature leading a supersaturated solid solution (SSS). This is followed by quenching, which meant the cooling of the material until room temperature in order to keep SSS even under low temperature. The goal is having a SSS under low temperature in order to provide the material a controlled growth of precipitates by warming up. This step is called aging and can be carried out either naturally or artificially. Natural aging usually takes place under room temperature and takes more time to get set. In artificially aging, the metal should be placed into a stove and takes less time to get set.

Table 2: Temper designations

<i>LETTER</i>	<i>MEANING</i>
F	As fabricated – Applicable to products of a forming process in which there is no special control
O	Annealed – Applicable to product which has been treated to produce lowest strength conditions to improve ductility and dimensions stability
H	Strain hardened – Applicable to product that gets strengthened through cold working
W	Solution heat treated – A non-stable temper applicable only to alloys which age spontaneously at room temperature after solution heat-treatment
T	Thermally treated – To produce stable tempers. Applies to products which has been heat-treated, sometimes with supplementary strain-hardening in order to produce a stable temper

Source: (AlcoTec, 2015)

Beyond temper designations shown above, there is still subdivisions of T temper, shown below.

- T1.....Naturally aged after cooling from high temperatures shaping process
- T2.....Cold worked after cooling from high temperatures shaping process and artificially aged afterwards
- T3.....Solution heat-treated, cold worked and naturally aged
- T4.....Solution heat-treated and naturally aged
- T5.....Artificially aged after cooling from high temperatures shaping process
- T6.....Solution heat-treated and artificially aged
- T7.....Solution heat-treated and stabilized (overaged)

T8.....Solution heat-treated, cold worked and artificially aged
T9.....Solution heat-treated, artificially aged and cold worked
T10.....Cold worked after cooling from high temperatures shaping process and artificially aged afterwards.

2.4.5 AA6082 – T6

Aluminium alloy is a medium strength alloy with high corrosion resistance. It has the highest strength among 6xxx alloys and presents good mechanical properties. The addition of large amount of manganese controls the grain structure which increases hardness of the material. It is easy to machine, which facilitates its use in the industry. As mentioned on page above, T6 means the alloy was solution heat-treated and artificially aged in order to control the grain size and achieve improvement of hardness and other mechanical properties. In Table 3 is shown the chemical elements and their percentage respectively and in Table 4 the mechanical properties.

Table 3: Chemical composition AA 6082 - T6

<i>CHEMICAL COMPONENTS</i>	<i>PENCENTAGE (%)</i>
Si	0,860
Fe	0,236
Cu	0,024
Mn	0,510
Mg	0,730
Cr	<0,014
Zn	0,021
Ti	0,020

Source: (NUTECH, 2011)

Table 4: Mechanical properties AA6082 - T6

<i>MECHANICAL PROPERTIES</i>	<i>VALUES</i>
UTS (MPA)	310
Hardness (Vickers)	95
Density (g/cm3)	2,7
YTS (MPA)	260

Melting point (°C)	550
Thermal conductivity (W/m-K)	170

Source: (MatWeb, 1996)

2.5 STEEL AND STAINLESS STEEL

2.5.1 GENERAL FEATURES

The development of the steel can be traced back 4000 years ago to the beginning of Iron Age. Proving being harder and stronger than bronze, which had been the most used metal, iron began to replace bronze on weaponry and tools.

By the nineteenth (19th) century, the amount of iron being consumed to expand railroads allowed metallurgists to figure out iron's brittleness and inefficient production processes. In 1906, Leon Guillet published researches on steel alloys; he also published a detailed study of an iron-nickel-chromium alloy, which is the basic metallurgical structure of 300 series steel alloys. In Germany, in 1908, Monnartz & Borchers found out evidences about relationship between a minimum level of chromium (10.5%) and corrosion resistance as well as importance of low carbon content and role of molybdenum in getting corrosion resistance increased.

Meanwhile, the discovery of stainless steel had started in the beginning of eighteenth (18th) century and was developed over the years.

Stainless steel is a steel alloy with minimum of 10.5% chromium of mass. It is widely applied in many industries because it does not neither corrode, rust nor stain water as ordinary steel does.

Dissimilarity between stainless steel and carbon steel can be noticed related to the amount of chromium present in the chemical composition. As long as stainless steel undergoes atmospheric pressure, an inert layer of chromium is formed gradually. Such layer prevents the interstitial diffusion of the oxygen.

2.5.2 STEEL DESIGNATIONS

Specifications for stainless steel was issued by (International, 2005) in order to standardize steel designations worldwide.

In the 1930`s and 1940`s, the American Iron and Steel Institute (AISI) and SAE were both involved in efforts to standardize such a numbering system for steels.

Nowadays, steel quotes and certifications commonly make reference to both SAE and AISI, not always with accurate differentiation. Carbon steels and alloy steels are designated by a four-digit number, where the first digit indicates the main alloying element(s), the second digit indicates secondary alloying elements, and last two digits indicate amount of carbon.

2.5.3 AISI 316Ti

Grade 316Ti has been traditionally specified by Germans as users as Werkstoff number 1.4571 and known as AISI 316Ti as well. 316 is an austenitic steel and rated as the second most important steel out of 300 series steels behind 304. 316 stainless steel contains an addition of molybdenum that improves corrosion resistance.

Related to 316L, the lower amount carbon version of 316 stainless steel, it contains chromium to prevent corrosion in the alloy. The presence of this element leads to precipitation of chromium carbide at the grain boundaries; resulting in the formation of chromium zones adjacent to the grain boundaries, (this process is called sensitization). These zones form a very thin film that protects the metal from corrosive environment, making the steel stainless.

Nevertheless, these zones play as local galvanic couples, leading local galvanic corrosion. In order to prevent this behavior, titanium is added to the steel matrix, which form titanium carbide over chromium carbide, lowering the content of carbon in the steel. This process is called intergranular corrosion.

Thereby, it is pointed out that the better corrosion resistance of AISI 316Ti comparing to either AISI 302 or 304 makes it very usual in engineering components and industry applications.

The chemical elements and mechanical properties of AISI 316Ti are shown in Table 5.

Table 5: Chemical composition AISI 316Ti

<i>CHEMICAL COMPONENTES</i>	<i>PERCENTAGE (%)</i>
C	0,052
Si	0,540
Mn	1,390
P	-

S	-
Cr	16,88
Ni	10,33
Mo	2,00
Al	-
Cu	0,449
Ti	0,319

Source: (NUTECH, 2011)

Table 6: Mechanical properties AISI 316Ti

<i>MECHANICAL PROPERTIES</i>	<i>VALUES</i>
UTS (MPA)	510 – 710
Hardness (Vickers)	155
Density (g/cm ³)	8,0
YTS (MPA)	>220
Melting point (Celsius)	1380
Thermal conductivity (W/m x K)	16

Source: (MatWeb, 1996)

2.6 ALUMINIUM/STEEL AND DIFFUSION BONDING

FSW steel and aluminium is a tricky task because the probe can be worn out by the contact between probe and steel sheet. If such contact takes place, probe lifetime will be shortened. Since the probe cannot be in contact with steel, the major challenge is to find suitable parameters to produce a sound joint. Since there is no metal addition in FSW, the bonding between dissimilar materials takes place through a metallurgical phenomenon called diffusion.

(D.Callister, 2007) pointed out that diffusion is a stepwise migration of atoms from lattice site to lattice site. For an atom to make such a move, two conditions should be found: there must be an empty adjacent site and (2) atoms must have enough energy to break down the bonds with its neighbour atoms and cause lattice distortion during

displacement. At specific temperature, depending on the material properties and microstructure, small fractions of total numbers of atoms is capable of diffuse. The higher is temperature, the higher is the atoms movements and the diffusion becomes more likely.

According to (D.Callister, 2007), there are two major diffusion methods: vacancy diffusion and interstitial diffusion. The bonding between aluminium and steel takes place mainly by interstitial diffusion due to great number of small spaces in aluminium matrix.

Table 7: Diffusion elements

DIFFUSION SPECIES	HOST METAL	D_0 (M ² /S)	ACTIVATION ENERGY		CALCULATED VALUE	
			Q_D		T (°C)	D (M ² /S)
			KJ/MOL	EV/ATOM		
Fe	α -Fe (BCC)	$2,8 \times 10^{-4}$	251	2,60	500	$3,0 \times 10^{-21}$
Fe	γ -Fe (FCC)	$5,0 \times 10^{-5}$	284	2,94	900	$1,1 \times 10^{-17}$
C	α -Fe	$6,2 \times 10^{-7}$	80	0,83	500	$2,4 \times 10^{-12}$
C	γ -Fe	$2,3 \times 10^{-5}$	148	1,53	900	$5,9 \times 10^{-12}$
Cu	Cu	$7,8 \times 10^{-5}$	211	2,19	500	$4,2 \times 10^{-19}$
Zn	Cu	$2,4 \times 10^{-5}$	189	1,96	500	$4,0 \times 10^{-18}$
Al	Al	$2,3 \times 10^{-4}$	144	1,49	500	$4,2 \times 10^{-14}$
Cu	Al	$6,5 \times 10^{-5}$	136	1,41	500	$4,1 \times 10^{-14}$
Mg	Al	$1,2 \times 10^{-4}$	131	1,35	500	$1,9 \times 10^{-13}$
Cu	Ni	$2,7 \times 10^{-5}$	256	2,65	500	$1,3 \times 10^{-22}$

Source: (D.Callister, 2007)

Table 3 and Table 5 show the atoms contained in AA6082-T6 and AISI 316Ti. First column of Table 7 indicates candidate atoms to be diffused under the effect of presented parameters above. For example, looking at Table 3 and Table 5 we can notice the presence of copper (Cu) in both alloys. Looking at fifth row of Table 7, there is Cu as diffusion specie and host metal. If the parameters shown on the third column onward are achieved during FSW (Table 7), host metal Cu hosts Cu (diffusion specie) and atomic diffusion takes place under a temperature of 500 °.

3 EXPERIMENTAL APPROACH

The design used for experiments was based on a preliminary parameters investigation. The three most analyzed parameters were rotation speed, translation speed and offset. Basic analysis was carried out initially considering superficial smoothness and defects.

After FSW, a characterization of the joint was performed. Such characterization includes microstructure analysis, hardness, bending and tensile tests. FSW experimental approach is described by the flow chart shown in Figure 7.

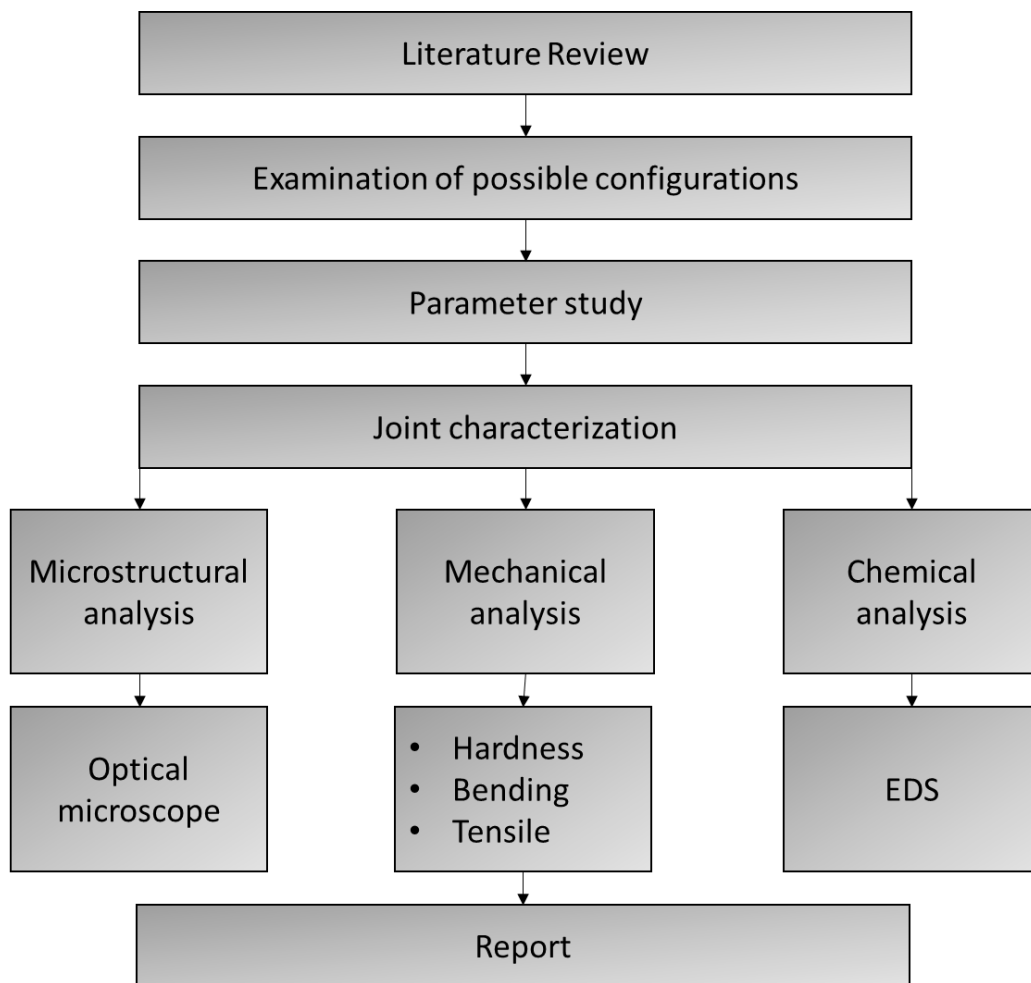


Figure 7: Chart flow displaying the procedure adopted

4 MATERIALS AND METHODS

4.1 MATERIALS

FSW was performed using a standard tool split in two different parts: probe and shoulder. Prior to FSW, these parts should be screwed to each other due to presence of forces and torque in FSW. The parts and assembly are shown in Figure 8.



Figure 8: Probe, shoulder and assembly

The threaded probe shown in Figure 8 and figured out in Section 2.1.5 enables better material flow, decrease welding forces and material volume that moves from AS to RS leading higher quality weld joints.

The dissimilar materials used were AISI 316Ti (Werkstoffe1.4571) and AA6082-T6. The addition of Ti (Titanium) in AISI 316L makes this steel more proper for naval industry, since this addition rises corrosion resistance (see Section 2.5.3) and this feature is fundamental during the lifetime of the vessel. Besides, AA6xxx alloy is one of most resistant and easier to weld wrought alloys. Therefore, the FSW of these alloys will provide suitable mechanical properties in order to meet the requirements of a naval structure.

As mentioned in Section 2.6, the stir between probe and steel plate should not take place because of probe wear in FSW. Therefore, there is no mechanical contact between

probe and steel sheet, which makes diffusion the major bonding mechanism between steel and aluminium.

Steel and aluminium sheets were equally dimensioned. Both presents 300 mm length, 150 mm width and 6 mm thickness. The sheets were placed on a backing bar and

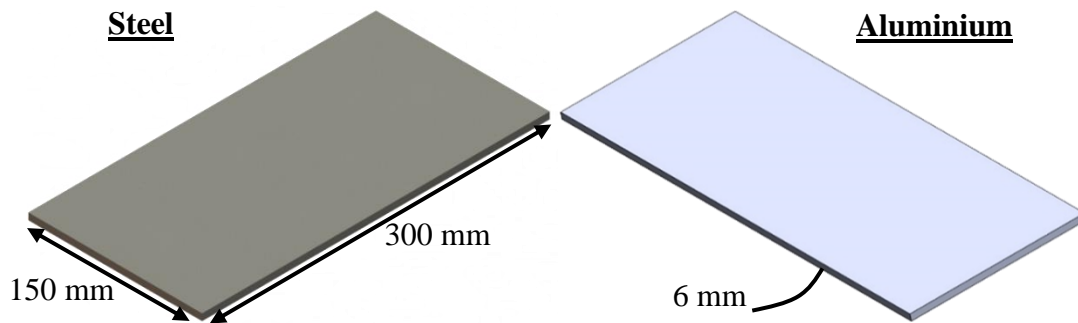


Figure 9: Main dimensions of steel and aluminium sheets

clamped afterwards.

4.2 METHODOLOGY

4.2.1 TOOL CONFIGURATION

In this work, a threaded probe with an edge angle of 12° was used. Aluminium and steel sheets were 12° machined in order to be in agreement with probe interface. Such joint configuration makes full contact between the interface and the probe leading more uniform material flow and temperature distribution on the top and bottom of the plates. Besides, the matching angle generates more plasticized material and increase the heat generation in steel-aluminium interface. Such configuration can be noticed in Figure 10.

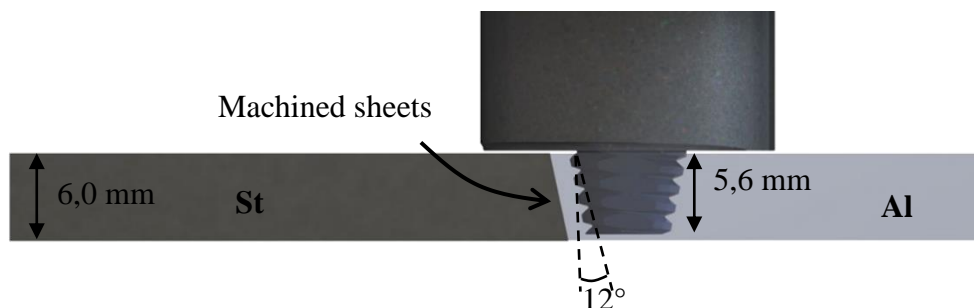


Figure 10: Joint configuration with 12° angle of the probe edge

In this figure, it is shown the probe fully dived within aluminium alloy. Section 2.1.4 points out that probe is not allowed to stir steel sheet because the pin can be worn out and its lifetime being shortened. Such effect in FSW forces the inclusion of one more

parameter to be consider: the offset. The offset can be defined as the distance between the probe edge and the Al/St interface (see Figure 3).

4.2.2 PARAMETERS STUDY

Besides the offset, the other input parameters at the machine were rotation speed (RPM), translation speed (mm/s), axial force (KN) and tilt angle (°). Probe and shoulder were defined previously and were not switched in this work.

Rotation speed was varied from 300 RPM to 1000 RPM, translation speed was set to 2.0 mm/s and 4.0 mm/s, axial force to 10.0 KN and 12.5 KN and offset ranged from 0.0 to 0.5 mm. These values were based on previous experiences, where (K.K.Ramachadran, N.Murugan, Kumar, & S.Shashi, 2015) pointed out that rotation speed from 300 until 1200 RPM and translation speed nearby 80 mm/min could produce sound weld joints for dissimilar materials using 3 mm AA5052 (aluminium) and hot rolled HSLA steel. Although the rotation speed range was used for 3mm plates, AA5052 is less resistant than AA6082-T6 used in this study. Therefore, in this work was decided to keep the same logic, starting with 1000 RPM until 300 RPM. (Ramachandran & Murugan, 2019) stated that axial force around 8 KN could generate joints with high strength using the same materials: 3mm AA5052 and hot rolled HSLA steel. Since the 8 KN axial force is fixed and the plate thickness in this work is 6 mm, the force was fixed in 10 and 12.5 KN. While (Song, Nakata, Wu, Liao, & Zhou, 2014) ranged the offset between 0.0 to 1.2 mm for FSWed butt joint of 2 mm AA6061 (aluminium) and Ti6Al4V (titanium) plates. In our study, the offset was varied from 0.0 to 0.5 mm, since this parameter is not directly related to the thickness, but actually to the materials properties and the heat input.

Table 8 presents the FSW parameters of each specimen used in this work.

Table 8: Parameters applied in FSW samples

Weld ID	Rotation speed	Translation speed	Axial Force	Offset
	[RPM]	[mm/s]	[KN]	[mm]
E1	1000	2.0	10.0	0.1
E2	1000	2.0	12.5	0.1
E3	700	2.0	12.5	0.1

E4	500	2.0	12.5	0.1
E5	500	4.0	12.5	0.1
E6	300	2.0	12.5	0.0
E7	300	2.0	12.5	0.1
E8	300	2.0	12.5	0.3
E9	300	2.0	12.5	0.5

4.2.3 FSW MACHINERY

The welds were carried out drawing upon Gantry System (see Figure 12) where all parameters were managed by an electronic system. The tool employed in this work was steel manufactured and capable of welding dissimilar materials as steel, aluminium, magnesium and copper. The sheets were clamped down using supports 300 mm long, 60 mm wide and 40 mm thick (see Figure 11).

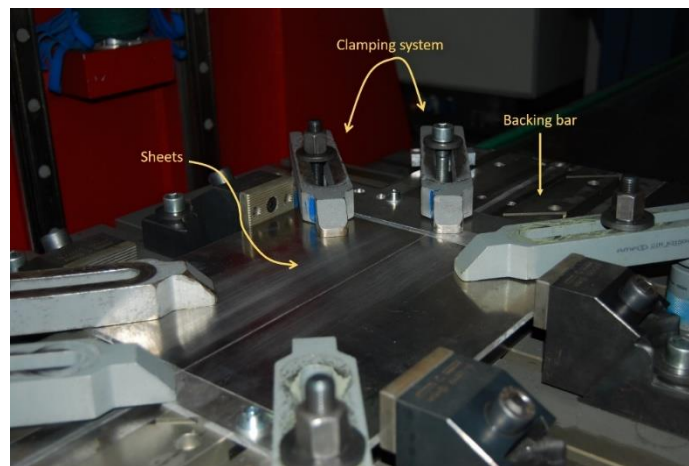


Figure 11: Clamping system

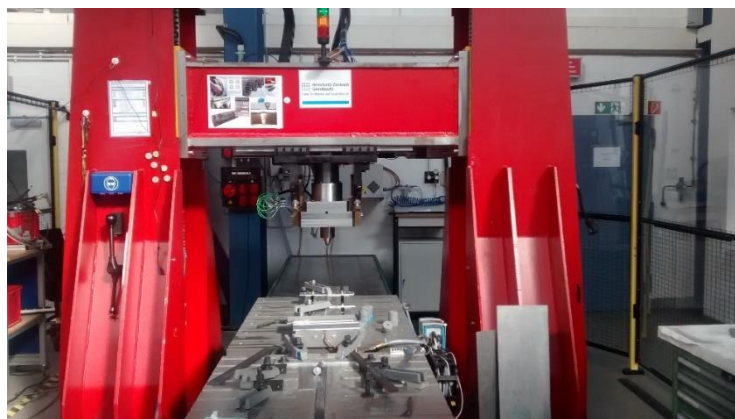


Figure 12: Gantry system for FSW

Prior to FSW, thermocouples were placed in pre-determinate position within aluminium and steel plates to measure the temperature along the weld seam. The thermocouples arrangement is shown in Figure 13.

4.2.4 MICROSTRUCTURE CHARACTERIZATION

The samples have been characterized by an optical microscopy to find eventual defects and microscopic characterization led by FSW. Metallographic samples were taken from a cross section cut off from the welded samples. According to (ISO, Friction stir welding of aluminium - General requirements (Part 3), 2006), the first and the final 50 mm of the weld should be ruled out and the leftover must be considered to infer the results. Small samples of 48 x 15 x 6 mm were cut to be analyzed in the optical microscope. The cutting machine used was a Struers Axitom-5 shown in Figure 14.

Afterwards, the samples were embedded in a 50 mm support made by cold curing resin, which is a mixture of Demotec 20 powder and Demotec 20 liquid with a 2:1 ratio

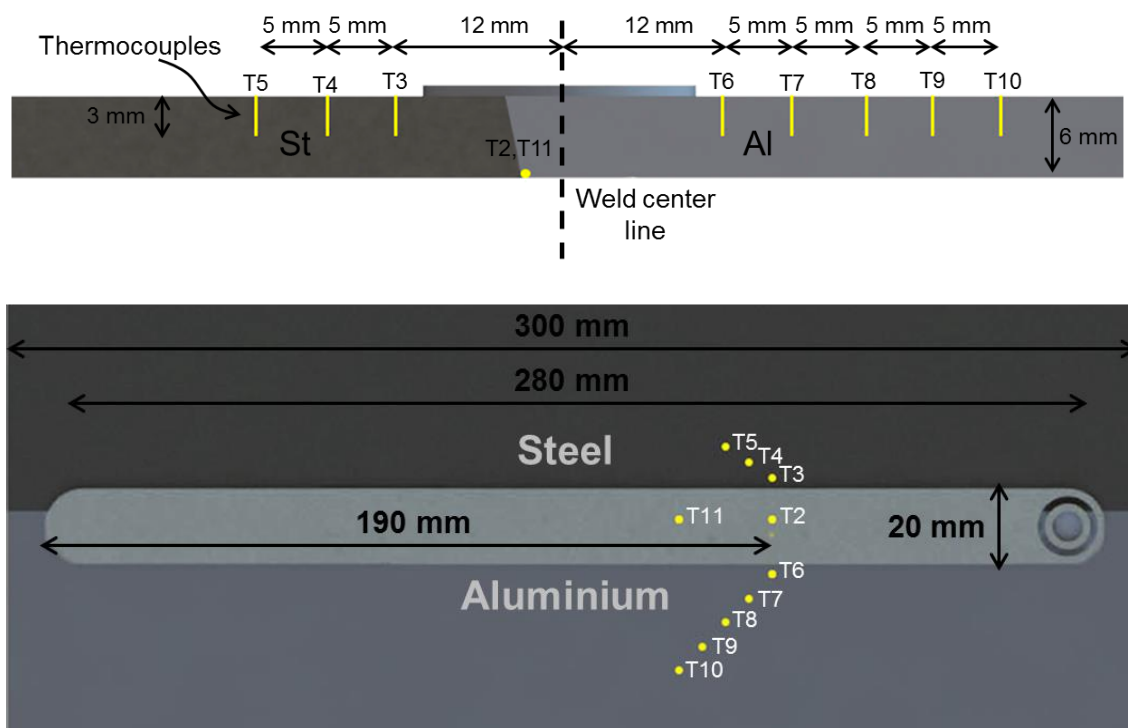


Figure 13: Thermocouples arrangement in transversal and longitudinal views, respectively. After cutting and embedding the samples, the next step was grinding and polishing the specimens in such a way to decrease the number of scratches on sample surface. The polishing machine is shown in Figure 16. Samples were etched with Barker solution for aluminium and Electrolytic etchant 10% oxalic acid for steel. The parameters were 25V during 90s for Barker etchant and 15V during 10s for Electrolytic etchant.

Metallographic preparation was performed using 320 and 800 sandpapers, polished with Diamond Suspension 9 μm , followed by Diamond Suspension 3 μm and Diamond Suspension 1 μm afterwards. Surface finish was carried out with OPS solution (50% OPS + 50% water) on the polishing machine (Figure 16). The clothes used are shown on Table 9.

Table 9: Grinding and polishing clothes used in FSW samples

	<i>STEP</i>	<i>LUBRICANT</i>
Grinding	Silicon carbide abrasive paper P320	Water
	Silicon carbide abrasive paper P800	Water
Polishing	MD Largo 9 μm	Struers DiaPro Dac
	MD Floc 3 μm	Struers DiaPro Dac
	MD Nap 1 μm	Struers DiaPro Dac
	MD Chem – OPS Solution	Destiled water



Figure 14: Cut-off machine



Figure 15: Leica optical microscope



Figure 16: Grinding and polishing machine

4.2.5 MICROHARDNESS CHARACTERIZATION

Vickers hardness test were carried out on a Zwick/Roell machine through TestXper software. The applied load was 0,2 Kgf during 10 s for all samples, as in accordance to (ISO, 2011). Hardness test was performed in the medium line of the sample (3 mm away from top and bottom) with a 300 μm indentation space.



Figure 17: Microhardness machine

4.2.6 BENDING AND TENSILE TESTS

The employment of new materials and methods inside shipbuilding industry requires a detailed, feasible and reliable datasheet of the material. In the information required, mechanical properties of these materials should be specified on the datasheet of the materials. In this direction, this work used mechanical experiments to determinate the mechanical properties of the aluminium/steel joint. The experiments carried out for analyzing weld mechanical properties were bending and tensile test.

They were carried out on a Zwick machine, which. Automation provided reliability and accuracy of the results. The specimens were designed according to (ISO, 2012, pp. 1-21) and (ISO, 2012, pp. 1-12) for bending and tensile, respectively.

4.2.6.1 BENDING TEST (BT)

The three-point bending test were performed to evaluate the penetration of the tool throughout the whole thickness. Three-point bending test is composed of a plunger and two dies, which ones works as supports for the specimens. The dies diameter was 46 mm, the distance between their center 89 mm and the plunger diameter 30 mm. The specimens were dimensioned according to (ISO, 2012, pp. 1-21), with 290 mm length, 24 mm width and 6 mm thickness. The specimens were 1mm machined on the bottom in order to avoid crack beginning on the bottom of the specimen, which region underwent tensile forces due to plunger penetration. Figure 18 shows bending test draft with the dimensions described above.

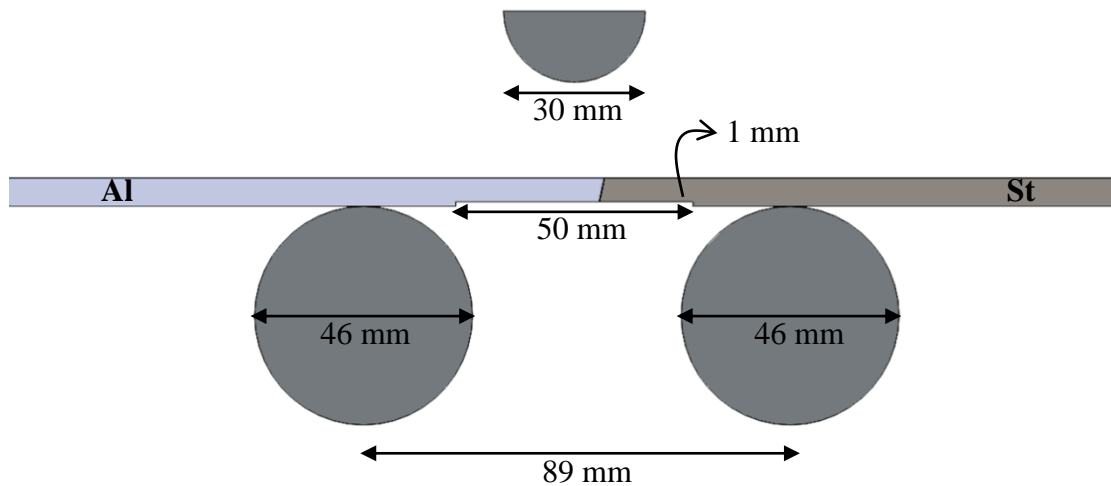


Figure 18: Draft of Bending test including specimen, plunger on the top and dies on the bottom (support of the specimens)

4.2.6.2 TENSILE TEST (TT)

Tensile specimens were carried out on a Zwick tensile machine. The specimens were dimensioned according to (ISO, 2012, pp. 1-12). They were machined as 212.50 mm long, and 37 mm wide on the shoulder. However, the cross-section area was shaped

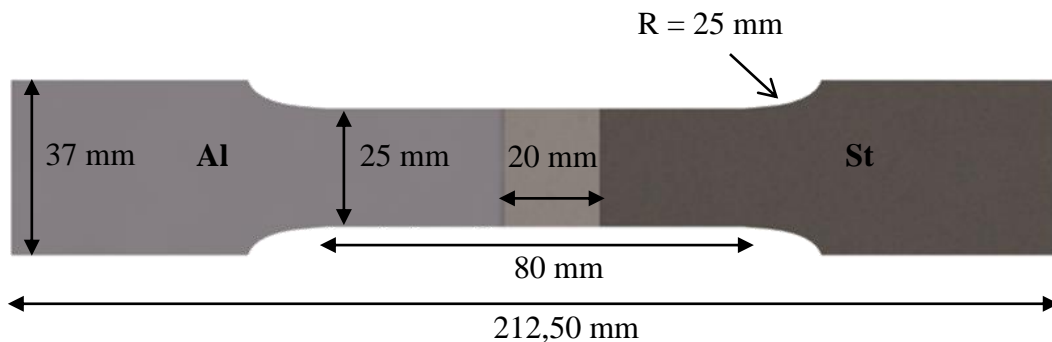


Figure 19: Draft of TT specimen

with dissimilar widths, as shown in Figure 19. Central region is 25 mm wide, while specimen shoulder is 37 mm. Specimen shoulder was overdimensioned because the wedge grips must be well supported on them to avoid slip during the test. Besides, an extensometer equidistant to the weld center line was used to measure the displacement of the grips and measure the strain.

According to (ISO, 2012, pp. 1-12), three specimens of each weld were tested in the tensile machine. The average and standard deviation of each weld will be shown in Table 12 in Section 5.

. The TT proceeding can be split in four main steps. First of all, the specimens are positioned and clamped on wedge grips (1). Afterwards, the extensometer is placed in such a way that its tips are equidistant to the weld center line (2). With the specimen stuck to the grips and the correct location of the extensometer, the parameters are set (3) and the test started (4). The parameters used in this work were 150 KN pre-load and 1 mm/s test speed. In Figure 20 is shown the specimen clamped by the grips and extensometer located nearby the weld seam.

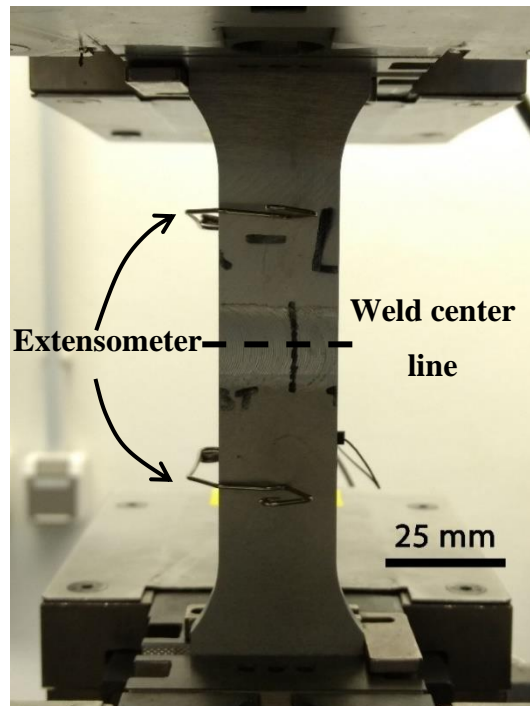


Figure 20: Example of TT showing the specimen clamped on the grips and the extensometer located on the front surface of the FSW sample

4.2.7 SCANNING ELECTRON MICROSCOPE (SEM)

A scanning electron microscope (see Figure 21) is a kind of electron microscope that produces images from a sample by scanning the surface with a focused beam of electrons. The electrons interact with atoms in the sample, which emit signals that contain information about sample's surface, topography and chemical components. The main objective of using SEM was to analyze chemical composition of aluminium/steel interface, IMC compounds thickness and steel particles analysis within aluminium alloy.

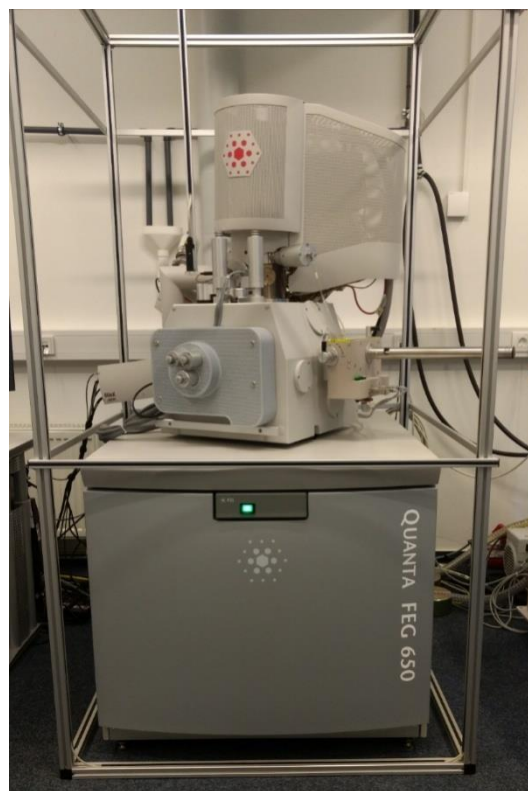


Figure 21: SEM machine

5 RESULTS AND DISCUSSIONS

5.1 WELD SURFACE

In fusion alloys, defects such as porosity, slags and cracks are usually associated with low-quality welds and weak mechanical properties. FSW usually does not produce these kinds of defect on the weld surface since there is no melting of materials. The plates are mechanically bonded due to the plastic deformation and the heat generation caused by the contact between the shoulder and the plate. Nevertheless, FSW is susceptible to other defects such as piping, tunnel and cracks. The top view of the weld surfaces are shown in Figure 22.

It can be observed that the specimens E1 (Figure 22a), E2 (Figure 22b) and E3 (Figure 22c) presented gaps and cracks along the entire weld seam. This result corresponds to the highest rotation speed, i.e., 700 RPM and 1000 RPM, which generated an unacceptable increase in the aluminium plate's temperature, preventing the desired bonding between the dissimilar materials.

A closer assessment of E6 shows lateral flash formation on the border of the seam (Figure 22f – upper part). When axial force is too high, the material is forced outside the welding zone. This expelled material is deposited on the border of the weld seam, resulting in flash generation. Although a lateral flash was formed, no cracks were noticed along the weld seam. Moreover, experiments E4 (Figure 22d), E5 (Figure 22e), E7 (Figure 22g), E8 (Figure 22h) and E9 (Figure 22i) did not present any superficial defects.

When the contact pressure between shoulder and workpiece is adequate, the material flows from AS and gets trapped in the RS due to a large drop in pressure. The high rotation speed of the tool triggers cylindrical cuts characterized by a multi-layer deposition over the weld seam, as discussed by (S.Muthukumaran & S.K.Mukherjee, 2008). Either too high or too low heat generation leads to the disappearance of the onion rings. It can be concluded that the parameters were sufficient to produce proper material flow leading to visible onion rings tracks and suitable weld surfaces.

Onion rings were formed along the joints in steel and aluminium plates' surfaces for all the experiments.

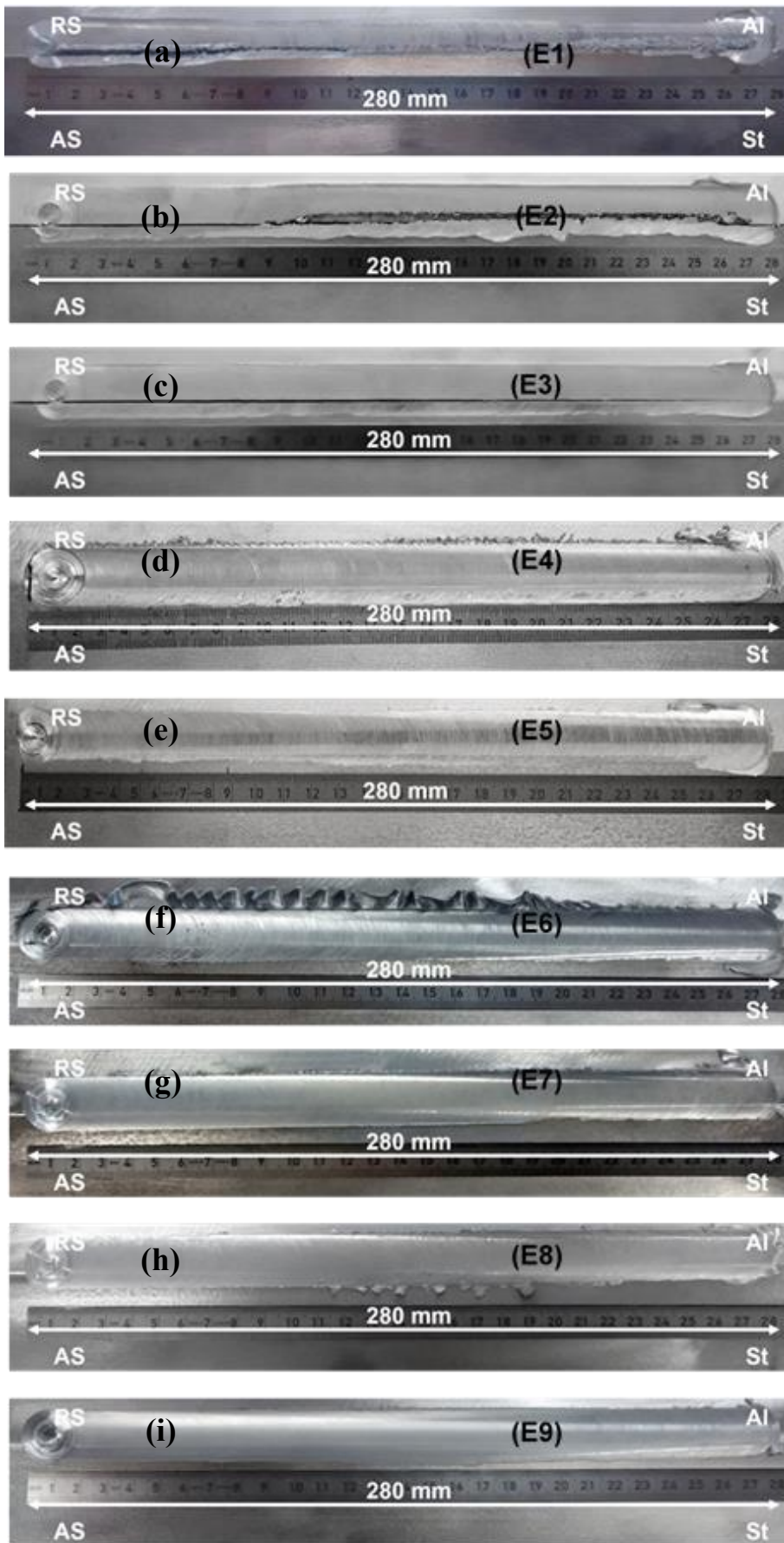


Figure 22: Top view of the weld seam for all experiments

5.2 TEMPERATURE DISTRIBUTION

The temperature distribution on FSW depends on energy input, heat loss to the backing bar and dwell time. A successful weld is widely influenced by the highest temperatures at the joint line of the plates (Hwang, Kang, Chiou, & Hsu, 2007). Temperature values *versus* time from starting point until end point inherent to the thermocouples T2 to T11 are shown in Figure 23 for experiment E7. T2, T6, T7, T8, T9, T10 and T11 were assembled on RS, while T3, T4 and T5 were placed on AS as shown in Figure 13. It can be noticed in Figure 23 that the temperatures are slightly higher around the end region than in the starting region. The build-up of heat in steel and aluminium plates and backing bar arising from friction is the major cause of this effect (Yau.Y.H., A.Hussain, R.K.Lalwani, K.H.Chan, & N.Hakimi, 2012).

It can be observed in Table 10 that the peak temperatures are significantly higher in the RS (aluminium) than in the AS (steel). The FSW probe fully immersed in the aluminium plate combined with displaced shoulder towards aluminium plate (see Figure 10) triggers more severe plastic deformation and friction at RS, which probably can explain these results. The highest observed temperatures occur in the thermocouples T2 and T11 due to their location in the aluminium plate at the vicinity of the interface, see Figure 13.

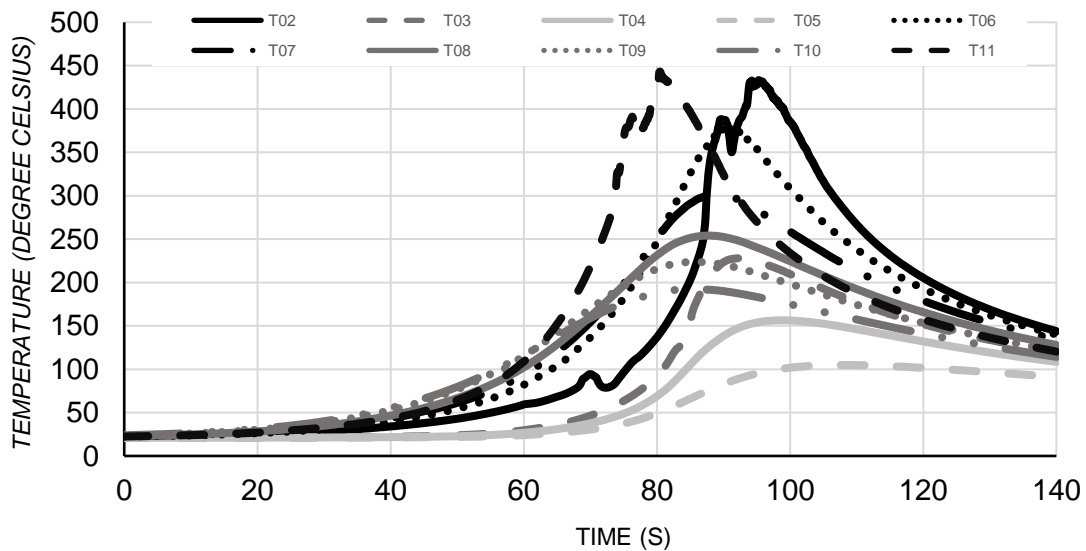


Figure 23: Temperature variation along time for thermocouples T2 up to T11 with temperature in Celsius and time in seconds

Table 10: Peak temperatures for thermocouples related to experiment E7

RS			AS		
ID	Time	Temp	ID	Time	Temp
	[s]	[°C]		[s]	[°C]
T11	80.5	443.2	T2	95.26	433.3
T6	90.63	379.8	T3	92.66	228
T7	89.62	301.8	T4	98.16	156.4
T8	88.02	254.1	T5	229.53	104.9
T9	85.42	223.7			
T10	85.42	192.5			

5.3 MICROSTRUCTURE

The values of the temperatures reached in the aluminium plate during welding plays an important role in FSW. Figure 24 shows a schematic view of SZ, TMAZ and HAZ in the aluminium sheet. As described in the next paragraphs, SZ can be defined as the mixture zone. It is the region where dynamic recrystallization occurs. TMAZ is a region that only exists in FSW. Such zone is where the grains are deformed in one direction but without recrystallization. HAZ is a typical zone to all welding process involving heat input. This region has no deformation and receives heat from stirring of the tool in the plates.

It can be observed in Figure 24a that the grains are fine and small in the aluminium stir zone (SZ), proving that dynamic recrystallization occurred during FSW.

The high plastic deformation in SZ is triggered by a sufficient stirring and contact between the tool and the plates. As result, a large number of crystals nuclei are produced, and the fine dynamic recrystallized grains are appearing (Weifeng & Xu, 2008).

Figure 24a shows a smooth transition between SZ and TMAZ. Such smooth and stepwise transition is a remarkable feature of RS in FSW, where the small grains of the SZ are progressively getting bigger in the TMAZ.

The TMAZ is a zone characterized by uniaxially deformed grains in one angular direction. The rubbing between probe and the material generates heat and plastic deformation without recrystallization of the grains. Meanwhile, the HAZ is the only welding zone that does not suffer from plastic deformation; but it is affected only by heat generation. Such a heat source leads to overgrowth of grains, which facilitates the movement of dislocations inside the HAZ, causing brittleness of the microstructure in this region.

Although a certain offset distance was applied in all experiments (see Table 8), the probe touches with the steel plate due to transverse forces that tend to move aluminium plate toward AS, (S. Muthukumaran, 2007). Such an effect led to equiaxed deformed grains without recrystallization for the steel microstructure, see Figure 24b. Thereby, such a deformed region can be considered-the steel TMAZ.

(Geronimo, Casarini, & Balancin, 2013) points out primary recrystallization of AISI 316L begins when temperature reaches approximately 1000°C. The highest measured temperature in the steel plate for experiment E7 was 228°C, which is not high enough to trigger recrystallization and to generate a SZ. The white dashed line observed in Figure 24b defines the limits of the TMAZ without SZ in the steel.

5.4 INTERFACE

As presented in the previous section, the friction and heat generation lead to microstructure changes throughout the whole thicknesses of aluminium and steel plates.

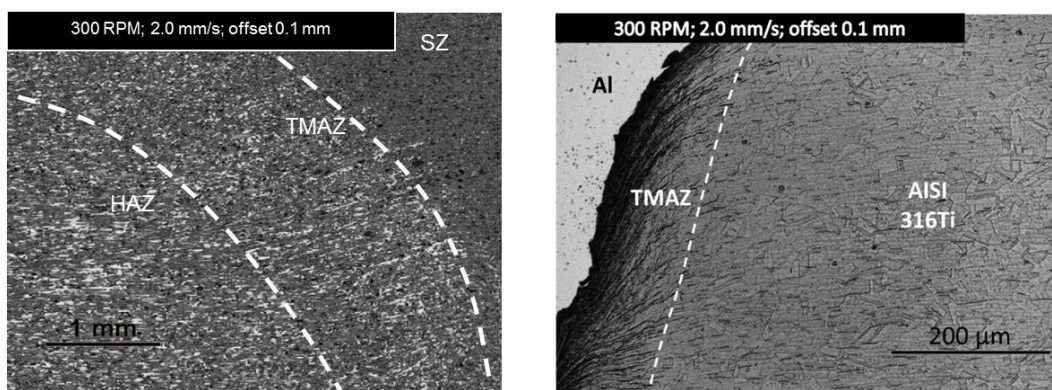


Figure 24: Aluminium and steel microstructure of welded joint in experiment E6

However, the offset distance is an important parameter that brings different characteristics of the joint.

In order to better understand the consequences of this parameter for the interface between the materials, a SEM analysis was performed. Figure 25 shows the SEM pictures corresponding to the upper part of the joint interface, while Figure 26 corresponds to the middle part of the joint.

During welding, when enough heat is produced, the stirring and pressure breaks the oxide layer of the aluminium and steel surfaces, leading to atomic bonding between them. Then, an IMC layer is formed, which works and behaves almost like the atomic bonding of both materials, (Hussein, Tahir, & Hadzley, 2015).

According to (Bozzi, A.L.Helbert-tter, T.Baudin, B.Criqui, & J.G.Kerbiguet, 2010) and (M.Yılmaz, M.Çöl, & M.Acet, 2002), there is an inverse correlation between the IMC thickness and the weld strength.

In Figure 25 and Figure 26, the grey region present in the left of the figure corresponds to the AISI 316Ti while the darkest region on the right corresponds to the AA 6082-T6.

The thickest IMC stripes of $0.97\ \mu\text{m}$ found in the experiment E6 at the upper part of the seam, see Figure 25a. As highlighted by (Lee, Schmoecker, Mercardo, Biallas, & Jung, 2006), the greatest plastic deformation take place close to the shoulder, causing more atomic diffusion than in other regions. It explains that IMC stripe thickening is observed in the upper part of the interface. However, the IMC layer disappears in the middle of the seams as shown in Figure 26a. Even the steel inserts are not surrounded by IMC in this figure.

Regarding the specimen E7, we can observe that an IMC layer is formed on both the upper and the middle part of the seam, as shown in Figure 25b and Figure 26b, respectively. However, the maximum thickness of the IMC, i.e., $0.75\ \mu\text{m}$ is observed for the upper part of the weld, while $0.27\ \mu\text{m}$ is identified at the middle part of the seam.

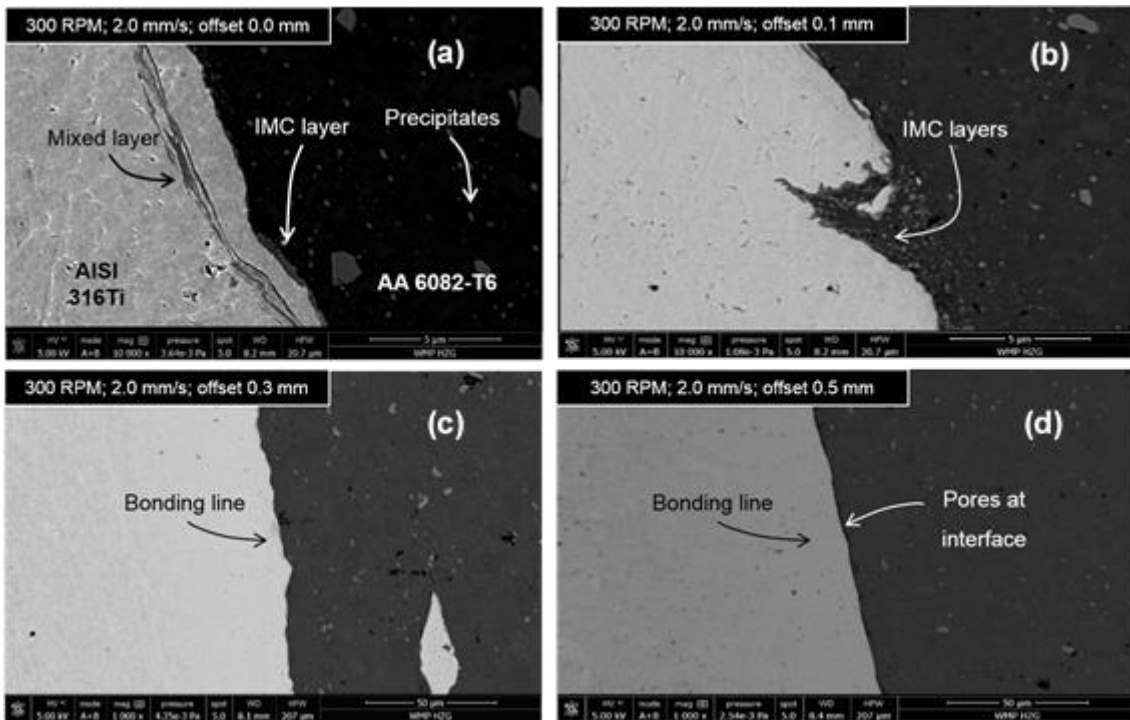


Figure 25: SEM pictures at the upper part of the joint corresponding to experiments E6, E7, E8 and E9

The complex structure of the IMC layers in experiment E7 is explained by the larger offset of the tool, i.e., 0.1 mm instead of 0.0 mm, which results in less stirring in the interface region. The greatest presence of IMC on the top indicates better stirring and mixing due to higher temperatures produced by the shoulder.

When the offset is even higher, i.e., 0.3 mm for the specimen E8, it is observed that the IMC layer almost disappeared from both upper and middle part of the seam (see Figure 25c and Figure 26c) although an atomic bonding of the interface is still observed.

Finally, when the offset is set to 0.5 mm (E9), it is clear that the bonding does no longer occur properly. Some pores are observed at the upper part of the seam and a void of around $6.2 \mu\text{m}$ is observed in the middle part. Pores and voids across the joint indicate bad stirring and weak temperature distribution due to the excessive offset applied. Since the probe was distant from interface, the heat generation was not enough to provide atomic diffusion and mechanical bonding across the joint line.

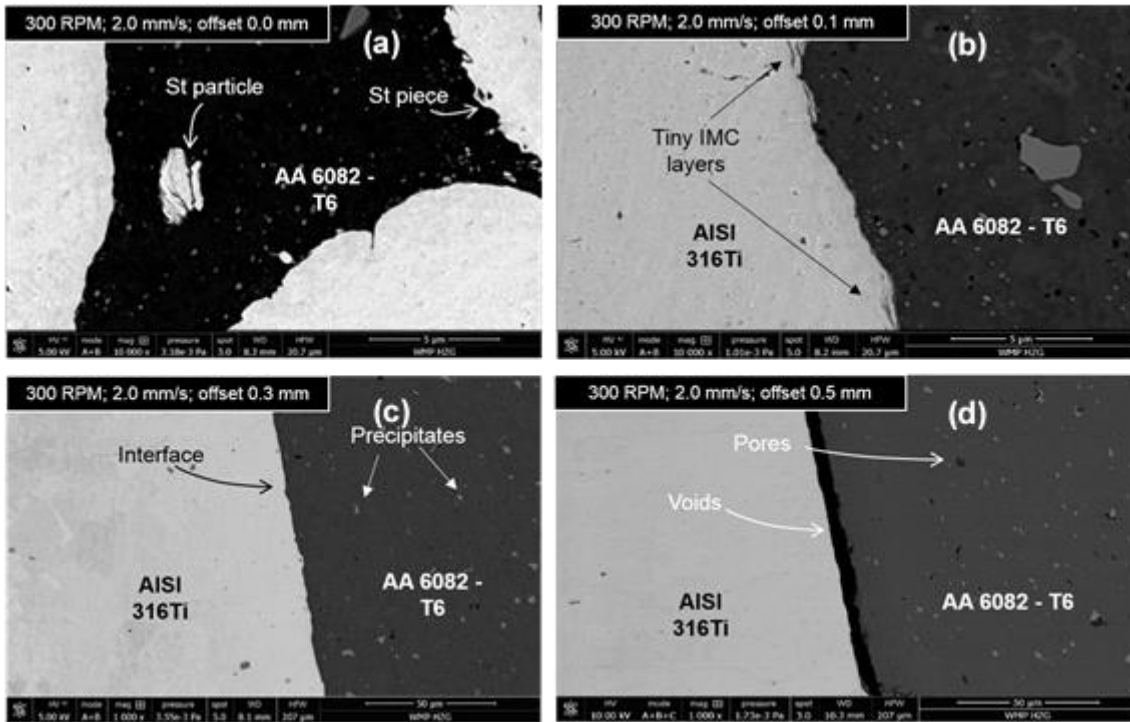


Figure 26: SEM pictures of the middle part of the joint corresponding to experiments E6, E7, E8 and E9

5.5 COMPOSITION OF THE STIR ZONE

The aluminium stir zone of the experiment E7 was analyzed using a field emission scanning electron microscope (FESEM). The samples were automatically grinded and polished beforehand.

As can be observed in Figure 27, during the welding of E7 the contact between the probe and the steel surface led to the release of steel particles from the interface spreading largely in the aluminium matrix.

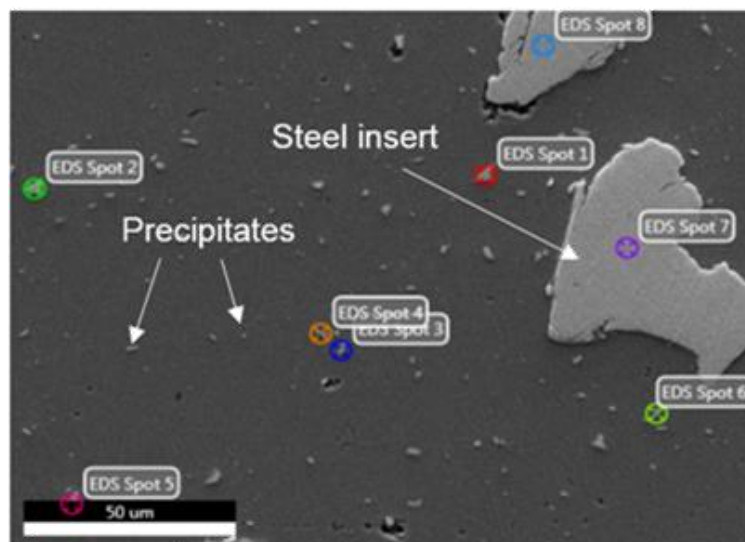


Figure 27: Steel inserts and precipitates within AA 6082-T6

The Table 11 shows the results of EDS analysis of the colour spots pointed out in Figure 27.

The EDS analysis of Spot 7 confirmed that the particle corresponds to a steel insert created by the severe friction between the probe and the steel. A similar situation is observed for spot 8. despite spot 1 presenting a different diagnostic. Indeed, the composition corresponds to an aluminium precipitate composed by 74.15% Al, 7.07% Si and 6.85% Mn. Similar results-were obtained for spots 2, 3, 4 and 6.

Table 11: EDS analysis for spots 1 and 7

Spot	Element	Weight	Atomic	Error
		[%]	[%]	[%]
1	AlK	61.75	74.15	2.16
1	SiK	6.13	7.07	4.63
1	MnK	11.62	6.85	5.77
7	MoL	2.05	1.20	16.99
7	CrK	17.90	19.23	4.45
7	FeK	69.95	69.96	3.18
7	NiK	10.10	9.61	7.98

5.6 MICROHARDNESS PROFILE ACROSS THE INTERFACE

Microhardness profiles were established in the middle of the plate thickness, i.e., 3 mm away from the top, throughout cross section of the welded joints. The measurements were taken using 300 µm indentation space and 0.2 Kgf force over 10s. The results of the measurements are presented in Figure 28.

The hardness values of the stirring zone of the aluminium present small peaks due to the presence of steel inserts and aluminium precipitates nearby the joint interface. Regarding the steel side, although the stirring zone does not exist, a higher hardness is

observed close to the interface. The black horizontal lines correspond to the hardness of the base material: 95 HV for AA 6082-T6 and 151 HV for AISI 316Ti.

As can be seen in Figure 28a, a similar behavior was observed for experiments E6 to E9. The hardness values are starting at the left side of the figure in the base metal region and then progressively decrease in the HAZ. A lower value of the hardness is usually observed in the HAZ due to the lack of plastic deformation and grain growth without recrystallization. It therefore makes the region more brittle due to ability of dislocations to move

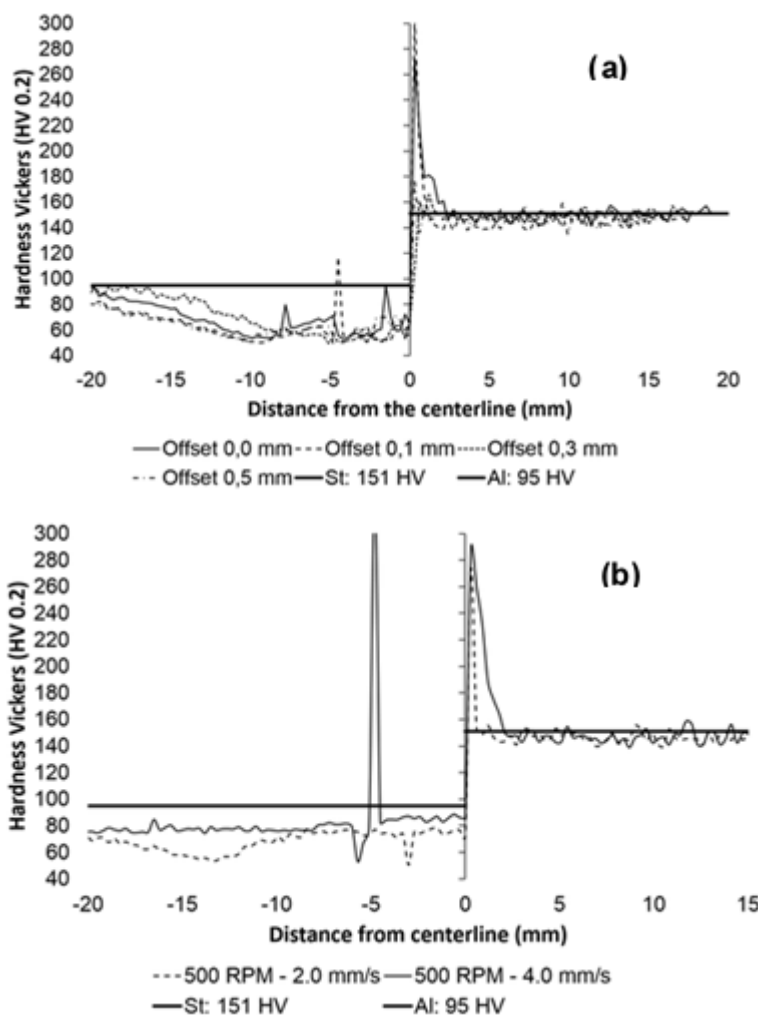


Figure 28: Microhardness Vickers across the welded joint interface where left side is Aluminium and right-side Steel – (a) E6 to E9 and (b) E4 and E5

In the stirring zone of the aluminium (left side of Figs.28a and 28b), the hardness values are slightly higher than in the HAZ but lower than in the base metal. High plastic deformation and dynamic recrystallization led to growth of new grains that were smaller and finer than in the base metal. These smaller and refined grains in this SZ explain the higher hardness values compared to the HAZ.

Regarding the experiments E4 and E5 (see Figure 28b), we can notice that the hardness values did not reach the base metal values at the aluminium side. A possible explanation is that the

temperature was not high enough to cause grain growth in HAZ; therefore, the hardness value remained unchanged up to the interface.

5.7 TENSILE TEST AND TOUGHNESS

The toughness modulus is known as the capacity of absorbing energy until fracture. This property is desirable for materials liable to collisions and impacts. Here, the toughness was calculated estimating the area below the tensile curve presented in Figure 29. The value of toughness and the ultimate tensile strength (UTS) are shown for specimens E4 to E9, in Table 12.

Of the six specimens, E6 and E7 obtained the two best tensile results with respectively a UTS of 198 MPa and 204 MPa and respectively a toughness of $8.66 \text{ MJ} \times \text{m}^{-3}$ and $8.65 \text{ MJ} \times \text{m}^{-3}$. Both E6 and E7 presented tensile fracture nearby HAZ at the aluminium side (see Figure 30a and Figure 30b) whereas the other parameters fractured at the joint's interface (see Figure 30c and Figure 30d).

Compared with these results, E8 and E9 present worst values for UTS and toughness as shown in Table 12. This can be explained by the fact that in both cases the bounding between the materials presented a smooth shape due to the higher value of the tool offset (see Figure 26c and Figure 26d). Also, the presence of voids observed at the interface of experiment E9 can be considered as an aggravating factor (see Figure 26d). As shown by (F. Beer, 2015) a curvy shape of the bounding line reduces the risk of crack propagation at the interface. Although UTS values are reasonable for E8 and E9, the toughness values show that these specimens did not absorb enough energy, leading to a short plastification regime. It explains why E6 and E7 had a lower offset of the tool and a curvy shape of the bonding interface (see Figure 26a and Figure 26b), performed better in terms of UTS and toughness.

(TsutomuTanaka, TaikiMorishige, & TomotakeHirata) and (M.Yılmaz, M.Çöl, & M.Acet, 2002) reported that the greater is tensile strength, the thinner the IMC layer for the inter-metallic interface. The outcome of this work goes in the same direction as E6 and E7 obtained the higher values of UTS and toughness simultaneously with the lower thickness of the IMC layer.

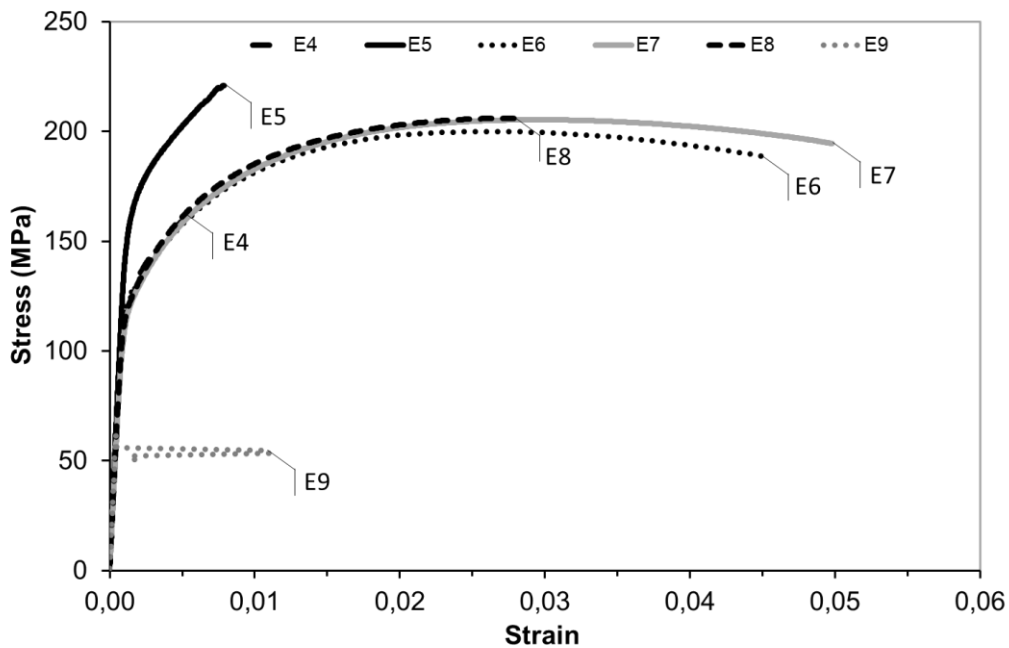


Figure 29: Tensile tests chart for experiments E4, E5, E6, E7, E8 and E9

5.8 BENDING TEST

Regarding the bending tests, a crack took place at the interface for all the experiments. The results of the bending tests are presented in Table 14 with the respective angles of crack appearance and break down of the samples.

Similarly to the tensile tests, experiments E6 and E7 performed better than the others with higher values of the angle until failure of, respectively, 161° and 162° . It corresponds to 90% of the maximum angle of 180° for bending tests (ISO, Destructives tests on welds in metallic materials - Bend tests, 2012).

On the other hand, the specimen E9 presents the worst result of all the experiments, achieving only 8° for the angle of failure, which represents 4.44% of the goal. From this result, it can be concluded that the largest offset of the tool, i.e., 0.5 mm, did not provide enough mixture between the two materials, leading in voids and pores around the interface.

5.9 COMPARISON WITH TRIPLATE®

As cited in Section 1, aluminium-steel joining is generally performed by the explosion method patented by Triplate® Shockwave Metalworking Technologies BV. Table 13 compares experiments E6 and E7 with the aluminium base metal and Triplate® UTS values. It is observed that the FSW process developed in this paper reaches around 60% of the UTS value of aluminium base metal, while the Triplate® achieves approximately 24%.

Table 12: Tensile test results with Toughness and UTS

Weld	Toughness	UTS	UTS percentage over aluminium
	[MJ x m ⁻³]	[MPa]	[%]
AA 6082 – T6 base material	NA	310	100
E4	0.86 ± 0.08	167.0 ± 1.5	53.9
E5	1.38 ± 0.15	215.8 ± 4.0	69.6
E6	8.66 ± 0.27	198.0 ± 1.8	63.9
E7	8.65 ± 0.74	204.3 ± 1.2	65.9
E8	3.77 ± 2.64	191.0 ± 25.3	61.6
E9	0.01 ± 0.02	96.8 ± 19.3	31.2

Table 13: Comparison between best FSW parameters and Triplate® Shockwave Metalworking Technologies BV

Weld	UTS	UTS percentage over Aluminium base material
ID	[MPa]	%
AA 6082-T6 base material	310	100
E6	198	63.9
E7	204	65.9
Triplate® Shockwave Metal Working	75	24.2

Table 14: Bending test results

Weld	Angle until crack takes place	Angle until break down
ID	[°]	[°]
E4	25	29
E5	NA	20
E6	12	161
E7	14	162
E8	30	43
E9	7	8



Figure 30: Fracture position of Tensile test: Al side for E6 and E7 and joint line for E8 and E9

6 CONCLUSION

This work proposed an analysis of the effects of FSW parameters joining a butt seam of two plates of 6 mm thickness of dissimilar materials AA 6082-T6 (retreating side) and AISI 316Ti (advancing side). A combination of rotation speed, translation speed, axial force and probe offset has been considered and organized in 9 experiments (E1 to E9).

Then, after a microstructure characterization, a comparison of mechanical properties has been carried out through tensile test, bending test and hardness test.

The following outcome are outlined below:

- The specimens (E1 to E3) corresponding to rotation speed (700 – 1000 RPM) did not produce a correct bonding between the materials due to a too high temperature
- The highest offset value for the probe does not create enough bonding between the plates due to the appearance of voids and pores at the interface.
- It has been proven that higher the strength of the joint the thinner is the IMC layer in the interface
- The highest joint strength has been obtained for the specimens (E6 and E7) having a rotation speed of 300 RPM, a translation speed of 2.0 mm/s, an axial force of 12.5 KN and an offset of 0.0 mm and 0.1 mm respectively. A strength of 198 MPa and 204 MPa has been achieved respectively for E6 and E7 corresponding to 63.9% and 65.9% of the aluminium base metal
- The best FSW joints experiments of this study presented an ultimate tensile strength at least twice higher than the actual industry standard that use explosion welding

Although FSW is not yet *the state of the art* in shipbuilding industry, the evidences show a great potential for joining steel and aluminium in large-scale production. However, further research is required to verify the behavior of the FSW of dissimilar materials to fatigue.

7 REFERENCES

- AlcoTec. (2015). *AlcoTec*. Fonte: www.alcote.com:
<http://www.alcotec.com/us/en/education/knowledge/techknowledge/understanding-the-alloys-of-aluminum.cfm>
- Association, T. A. (2015). *International Alloy Designations and Chemical Compositions Limits for Wrought Aluminium and Wrought Aluminium Alloys*. Arlington: The Aluminium Association.
- Bozzi, S., A.L.Helbert-tter, T.Baudin, B.Criqui, & J.G.Kerbiguet. (2010). Intermetallic compounds in Al6016/IF steel friction stir spot welds. *Material Science*.
- D.Callister, W. (2007). Diffusion. Em W. D.Callister, *Materials Science and Engineering* (pp. 109-130). Danvers: John Wiley and Sons, Inc.
- F. Beer, J. E. (2015). *Mechanics of Materials*. McGraw-Hill Education.
- G. Wang, Y. Z. (2018). Friction stir welding of high-strength aerospace aluminum alloy and application in rocket tank manufacturing. *Journal of Materials Science & Technology*, pp. 73-91.
- Geronimo, Casarini, F. H., & Balancin, O. (2013). Competition between dynamic recuperation and recrystallization of ASTM F138 Austenitic stainless steel utilized in medical devices. *Tecnol.Metal.Material.Mineral*, pp. 162-169.
- Hussein, S. A., Tahir, A. S., & Hadzley, A. (2015). Characteristics of aluminium-to-steel joint made by friction stor welding: a review. *Materials Today Communication*, pp. 32-49.
- Hwang, Y.-M., Kang, Z.-W., Chiou, Y.-C., & Hsu, H.-H. (2007). Experimental study on temperature distribution within the workpiece during friction stir welding of the aluminium alloys. *Machine tools & Manufacture* , pp. 778-787.
- International, A. (2005). Standard specification for stainless steel and shapes. Em A. International. West Conshohocken: ASTM Internation.
- ISO. (2006). *Friction stir welding of aluminium - General requirements (Part 3)*. ISO.
- ISO. (2011). *Destructive tests on welds in metallic materials - Hardness testing*. Berlin: ISO.
- ISO. (2012). *Destructive tests on welds in metallic materials - Bend tests*. Berlin: ISO.

- ISO. (2012). *Destructive tests on welds in metallic materials - Transverse tensile test (ISO 4136:2012)*. Berlin: ISO.
- ISO. (2012). *Destructives tests on welds in metallic materials - Bend tests*.
- K.K.Ramachadran, N.Murugan, Kumar, & S.Shashi. (2015). Effect of tool axis offset and geometry of tool pin profile on the characteristics of friction stir welded dissimilar aluminium alloy AA 5052 and HSLA steel. *Materials Science and Engineering*, pp. 219-233.
- Lee, W.-B., Schmoecker, M., Mercardo, U. A., Biallas, G., & Jung, S.-B. (2006). Interfacial reaction in steel-aluminium joints made by friction stir welding. *Scripta Materialia*, pp. 355-358.
- Liu, X., Lan, S., & Ni, J. (2014). Analysis of process parameters effects on friction stir welding of dissimilar aluminium alloy to advanced high strength steel. *Materials and Design*, pp. 50-62.
- M. Haghshenas, A. G. (2018). Joining of automotive sheet materials by friction-based welding methods: A review. *Engineering Science and Technology*, pp. 130-148.
- M.Movahedi, A.H.Kokabi, Reihani, S. S., & H.Najafi. (2011). Mechanical and Microstructural Characterization of Al-5083/St-12 lap joints made by friction stir welding. *Procedia Engineering*.
- M.Yılmaz, M.Çöl, & M.Acet. (2002). Interface properties of aluminum/steel friction-welded. *Materials Characterization*.
- MatWeb. (1996). *MatWeb - Material property data*. Fonte: matweb.com:
<http://matweb.com/search/DataSheet.aspx?MatGUID=fad29be6e64d4e95a241690f1f6e1eb7&ckck=1>
- NUTECH. (2011). *Vorabexemplar unverbindlich*. Geesthacht: NUTECH GMBH.
- P.Beer, F., & Johnston, E. (1996). *Mechanics of Materials*.
- R.S.Mishra, Z. (2005). Friction stir welding and processing. *Material Science and Engineering*.
- Ramachandran, K. K., & Murugan, N. (March de 2019). Influence of Axial Force on Tensile Strength and Microstructural Characteristics of Friction Stir Buttwelded Aluminum Alloy/Steel Joints. *Strength of Materials*, pp. 300-316.

- S. Muthukumar, S. K. (2007). Multi-layered metal flow and formation of onion rings in friction stir welds. *The International Journal of Advanced Manufacturing Technology*, pp. 68-73.
- S.Bozzi, A.L.Helbert-Etter, T.Baudin, B.Criqui, & J.G.Kerbiguet. (2010). Intermetallic compounds in Al 6016/IF-steel friction stir spot welds. *Materials Science and Engineering*.
- S.Muthukumar, & Mukherjee, S. (10 de July de 2007). Multi-layered material flow and formation of onion rings in friction sitr welding. pp. 68-73.
- S.Muthukumar, & S.K.Mukherjee. (2008). Multi-layered metal flow and formation of onion rings in friction stir welds. *Int J Adv Manuf Technol*.
- Scupin, P.-J. (2015). *Semi-stationary shoulder bobbin tool: a new approach in high speed friction stir welding*. Kiel: Peer-Jorge Scupin.
- Song, Z., Nakata, K., Wu, A., Liao, J., & Zhou, L. (2014). Influence of probe offset distance on interfacial microstructure and mechanical properties of friction stir butt welded joint of Ti6Al4V and A6061 dissimilar alloys. *Materials & Design*, pp. 269–278.
- Taban, E., Gould, J. E., & Lippold, J. C. (2010). Dissimilar friction welding of 6061-T6 aluminum and AISI 1018 steel: Properties and microstructural characterization. *Materials and Design*.
- Technologies, S. M. (s.d.). Aluminium/Steel transition joint.
- TsutomuTanaka, TaikiMorishige, & TomotakeHirata. (s.d.). Comprehensive analysis of joint strength for dissimilar friction stir welds of mild steel to aluminum alloys. *Scripta Materialia*, pp. 756-759.
- W.M, T., E.D.Nicholas, & S.D.Smith. (2001). Proceeding of the TMS 2001. *Aluminium Automotive and joining Sessions*, (p. 213).
- Watanabe, A. Y., & Takayama, H. (2006). Joining of aluminum alloy to steel by friction stir welding. *Journal of Materials Processing Technology*.
- Weifeng, & Xu, L. (2008). Temperature evolution, microstructure and mechanical properties of friction stir welded thick 2219-O aluminium alloy joints. *Materials and Design*, pp. 1886-1893.

- Y. Helal, Z. B. (2019). Microstructural evolution and mechanical properties of dissimilar friction stir lap welding aluminum alloy 6061-T6 to ultra low carbon steel. *Energy Procedia*, pp. 208-215.
- Y. Huang, T. H. (2019). Material flow and mechanical properties of aluminum-to-steel self-riveting friction stir lap joints. *Journal of Materials Processing Technology*, pp. 129-137.
- Yasuhiko, & Tanaka, K. (2009). Morphology of Compounds Formed by Isothermal Reactive Diffusion between solid Fe and Liquid Al. *Materials Transactions*, pp. 2212-2220.
- Yau.Y.H., A.Hussain, R.K.Lalwani, K.H.Chan, & N.Hakimi. (2012). Temperature distribution study during friction stir w. *International journals of Minerals, Metallurgy and Materials*, pp. 779-778.